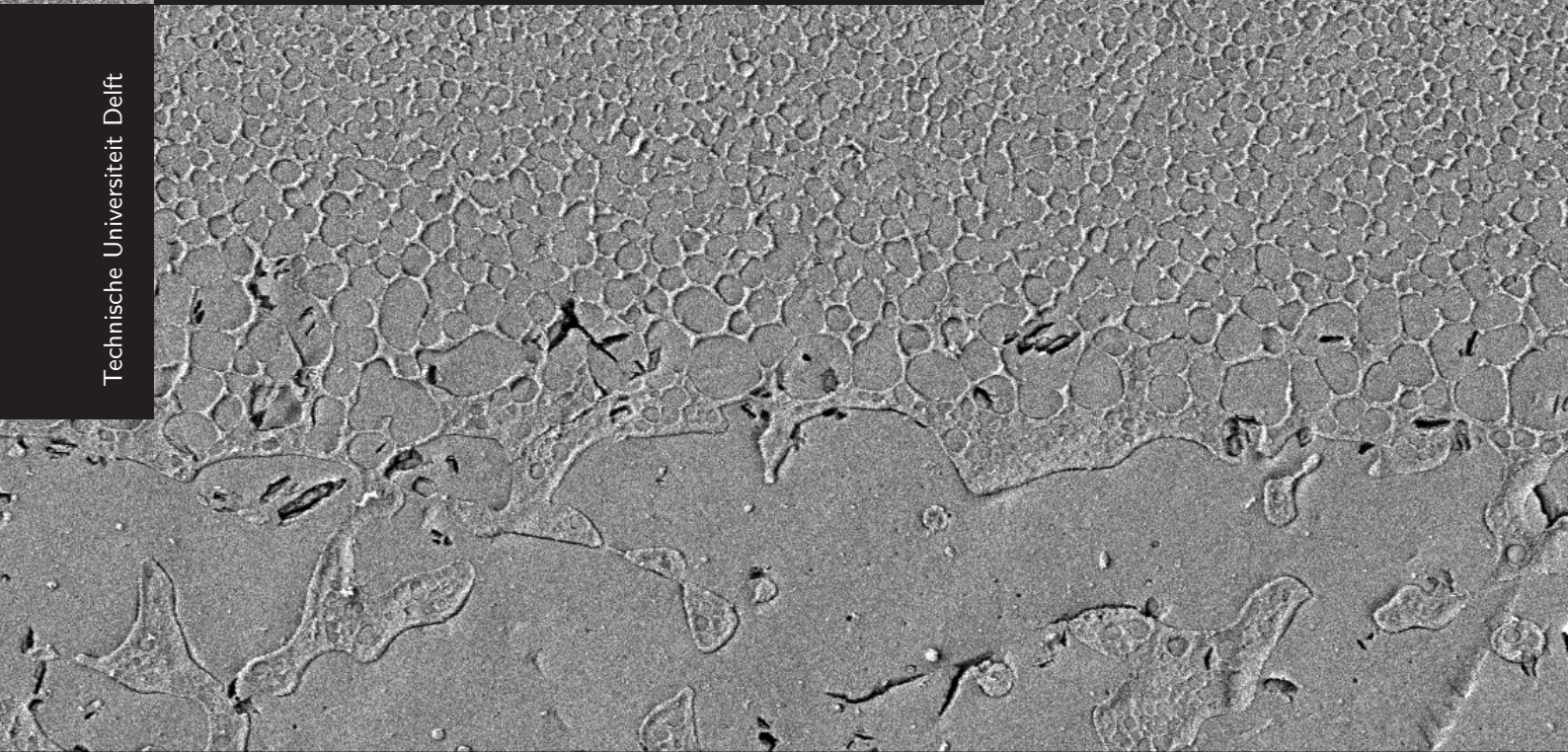


Welding of thermoplastic to thermoset composites through a thermoplastic interlayer

MSc. Thesis by Régis Van Moorlegem

Technische Universiteit Delft



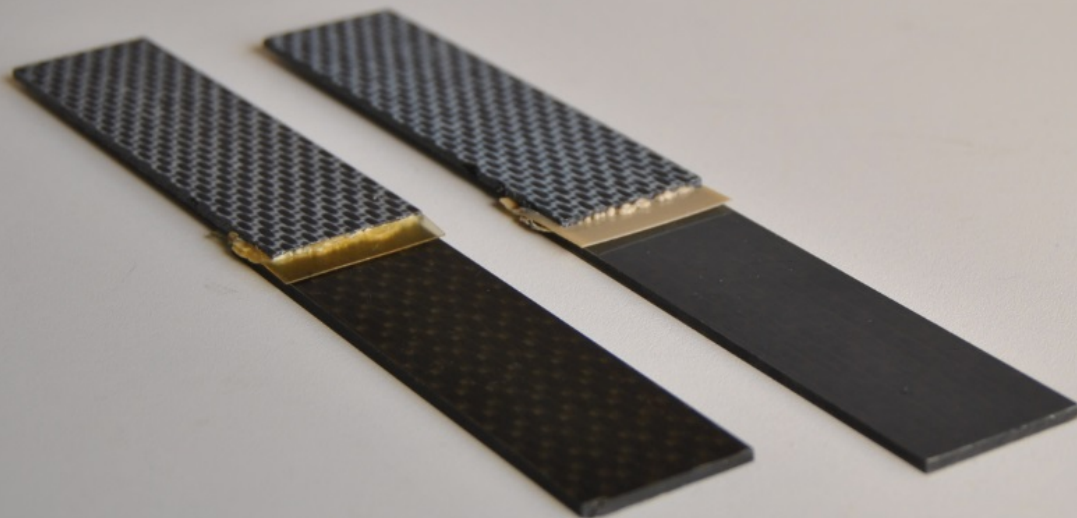
X 2,000

5.0kV LEI

10µm JEOL

SEM

WD 8mm



Welding of thermoplastic to thermoset composites through a thermoplastic interlayer

by

Régis Van Moorleghem

in partial fulfilment of the requirements for the degree of

Master of Science
Aerospace Engineering

at the Delft University of Technology,
to be defended publicly on Thursday June 2, 2016 at 13:00.

Supervisor:	Dr.ir. I. Fernandez Villegas	
Thesis committee:	Prof. R. Benedictus	Delft University of Technology
	Dr. ir. J. van Campen	Delft University of Technology
	Dr. ir. I. Fernandez Villegas	Delft University of Technology

Abstract

*Régis Van Moorleghem
Delft, May 2016*

Currently the joining of cured thermoset composite materials for aerospace applications occurs in a sub-optimal manner. The structure is joined by mechanical fastening, optionally in conjunction with an adhesive. The joining is sub-optimal because the fasteners require holes in the thin fibrous structure. These holes are stress concentrations, therefore the number of plies and thus the weight of the structure is increased to accommodate them. Adhesive joints do not require holes but these joints still have challenges in the field of non-destructive testing (NDT), which precludes their use for the joining of structural parts in aerospace. Consolidated thermoplastic materials have an additional joining technique that can be used, namely fusion bonding. This technique uses the property that distinguishes thermoplastics from thermosets, they have the ability to melt or soften under increased temperature. In this molten or softened state the molecular chains of the thermoplastic resin possesses increased mobility. If the thermoplastic is in intimate contact with another miscible thermoplastic while it is in this heated state the molecular chains can diffuse into each other and intermingle, creating a bond. This bond does not possess the stress concentrations associated with mechanical fastening, or the phenomenon of kissing bonds which inhibits certification in adhesive bonds.

In industry fusion bonding is solely applied to unreinforced thermoplastic materials, fusion bonding of thermoplastic composites is only applied in research. To enable fusion bonding of cured thermoset composites a thermoplastic interlayer can be co-cured, which is a thin thermoplastic film that provides a fusible surface to the thermoset structure, it can thus be used to fuse the thermoset structure to another fusible part. The interlayer can be surface treated before cure so that they can form an interfacial adhesive bond with the thermoset laminate. This approach makes the joint susceptible to the same challenges faced by adhesive bonding. Therefore this research investigates the use of a material combination that is initially miscible, so that they can form an interphase during cure instead of an adhesive interface, the interphase is a gradual transition from one material to the next .

The fusion bonding process itself also poses some challenges. Fusion bonding of aerospace grade thermoplastics typically require temperatures far above the maximum temperature allowed by the co-cured thermoset laminate. A solution to this problem is the use of a fast and concentrated method of heat generation that can keep the elevated temperature experienced by the thermoset material limited and short in time, preventing thermal degradation. Ultrasonic welding is a fusion bonding technique that is capable of creating fusion bonds with heating times in the order of 500ms, proven to be short enough to prevent thermal degradation for the materials used in this research. Another important issue foreseen and addressed in this research is the question if the interphase between the interlayer and the thermoset material can withstand the aggressive welding process. Previous experience with surface treated interlayers showed that some interlayer/surface treatment/thermoset material combinations can detach at the interlayer/thermoset interface after welding.

This research shows that the interphase is affected in some locations, but the fusion bond is nonetheless maintained through the entire weld overlap. The apparent lap shear strength of the joints created with an interphase forming interlayer is comparable to the joints created with adhesive interface forming interlayer. Both joint types retain their strength when exposed to prolonged exposure to moisture, simulating a worst-case scenario in a manufacturing setting. Exposure to a cleaning solvent significantly affected the interphase forming joint type, attributed to the amorphous structure of the thermoplastic used.

This research shows that when selecting the right material as interlayer for creating a fusion bonding capable thermoset laminate, a joint can be created that could avoid the certification challenge experienced by adhesive bonding, while simultaneously using aerospace grade materials without thermally degrading the joint during fusion.

Acknowledgements

In the second year of primary school I was walking on the playground, thinking, these kids from the 5th grade must have their head full with difficult equations, involving all kinds of letters and numbers, they must be so smart. At the time meester Bart, always keeping up the spirit with his guitar, was teaching us the first steps in math, involving wooden blocks representing single and double digit numbers. In the 5th grade we learned the relation between the circumference of a circle and its diameter, the magic pi. In secondary school I got interested in the STEM courses, a memorable moment was Mr. Verdonck, his face becoming a ripe tomato in the effort of shaking a container with small balls to represent the behaviour of atoms as a gas, or the time when he sprayed water through the whole classroom out of a syringe with multiple outlets, to demonstrate that pressure is distributed equally in all directions. The courses on electricity by Mr. Vanhoeylant during electromechanical engineering was lectured by every reference to Duvel imaginable, while the courses of Mr. Lensen on 3D modelling and FEM and the courses of Mr. Smet on metallurgy and welding were enlightened through their great personality.

I would like to thank inspiring teachers, for encouraging and motivating students in their subject. I would also like to express my sincere gratitude to my parents, Koen Van Moorleghem and Pascale Van Gijssels and my sister, Maryline for supporting me through my career as a student, especially during primary school. To dr.ir. Irene Fernandez Villegas, for inspiring me to pursue knowledge and competence in manufacturing of composite structures in her lectures, and her guidance and advice through this research. To Dr. Groves for introducing me to my girlfriend, Guyonne Alleman. To Guyonne, for her love and support. To my family and close friends, each for their own reasons. And last but not least to my cat, for keeping me company and providing friendship during the many hours of sitting behind a desk.

Régis Van Moorleghem

Contents

I	Research design	1
1	Introduction	3
1.1	Literature review	3
1.1.1	Joining of thermoplastics with thermosets	3
1.1.2	Ultrasonic welding	4
1.1.3	Interphase formation mechanism	5
1.1.4	Interphase evaluation methods	7
1.1.5	Material selection	9
1.1.6	The manufacturing environment	9
1.2	Research questions and objectives	10
2	Experimental	13
2.1	Materials	13
2.1.1	Polyether ether ketone	13
2.1.2	Polyetherimide	13
2.1.3	Carbon reinforced Hexply M18/1	14
2.2	Manufacturing	14
2.3	Conditioning	15
2.4	Evaluation methods	16
2.4.1	Microscopy and vibrational spectroscopy	16
2.4.2	Physical testing	17
2.4.3	Mechanical testing	17
II	Experiments, results & discussion	19
3	Investigations in weldable thermoset materials	21
3.1	Interphase assessment techniques	21
3.1.1	Microscopy analysis	21
3.1.2	Raman spectroscopy	24
3.1.3	Other techniques	25
3.1.4	Conclusion	26
3.2	Morphology of the interphase	27
3.2.1	Morphology of the M18 resin	27
3.2.2	Morphology of M18/PEEK interface	27
3.2.3	Morphology of M18/PEI interface	28
3.2.4	Conclusion	31
3.3	Influence of welding on the thermoplastic-thermoset connection	32
3.4	Co-curing of stiffeners	34
3.5	Conclusion	35
4	Welded joints	37
4.1	Determination of optimum welding parameters	37
4.2	Performance at dry/RT	38
4.3	Reducing the unwelded zones	41
4.4	Performance in a manufacturing environment	44
4.4.1	Exposure to water	44
4.4.2	Exposure to MEK	45
4.4.3	Exposure to contaminants	47
4.5	Conclusion	47

III	Conclusions and recommendations	49
5	Conclusion	51
6	Recommendations	53
	Bibliography	55

I

Research design

1

Introduction

1.1. Literature review

1.1.1. Joining of thermoplastics with thermosets

The long-term goal in the research area where this thesis contributes is to weld a carbon fibre (CF) PEEK bracket to a CF thermoset (TS) skin for aerospace applications. Of the three major joining technologies for cured or consolidated composite structures, namely mechanical fastening, adhesive bonding and fusion bonding only mechanical fastening and adhesive bonding can directly join a fully cured thermoset composite part [1]. Mechanical fastening requires the creation of holes, which introduces stress concentrations in the fibrous structure of composites. On the other hand adhesive bonding requires extensive surface preparation [2] and the phenomenon of weak bonds still pose a challenge in NDT inspection [3]. This leads to the fact that bonded joints need to be used in conjunction with mechanical fasteners for aerospace certification [3]. The direct use of fusion bonding is only possible for thermoplastic composites [1]. This is because fusion bonding uses the melt or softening capability of the thermoplastic material, a property which thermoset materials do not possess. The melting or softening increases molecular chain mobility, enabling interdiffusion of the thermoplastic molecular chains of the joint constituents when they are in intimate contact [4], creating a fusion bond.

Fusion bonding of cured thermoset (TS) structures can be achieved indirectly through the use of a thermoplastic (TP) interlayer or medium layer [1], which provides a fusible surface to the thermoset part. A strong attachment of this thermoplastic interlayer to the thermoset material is identified as the first challenge in fusion bonding with thermoset composites [1, 5]. TP/TS material combinations that are capable of interdiffusion can be directly co-cured, upon which they can form an interphase, this is discussed in subsection 1.1.3. Alternatively the materials can form an adhesive interface, the materials attach to each other via a selection of or a combination of mechanical interlocking, molecular bonding (Van der Waals forces and other chemical interactions) and/or a thermodynamic mechanism (minimal surface energy), discussed in detail in [6]. Chemical constraints can be avoided by using a hybrid interlayer [7], which is a woven fabric impregnated with TP through half the thickness, a challenging process. The other half sinks into the vitrifying thermoset resin during cure, creating a mechanical link between the two materials. Lastly research at the TU Delft [8, 9] explored the possibility to forego the interlayer by applying a surface treatment to the thermoset adherend to enable mechanical interlocking between the thermoset adherend and the thermoplastic resin of the joined part. This research aims to create a fusion bonded joint that could be certified in the future and is relatively cost effective in manufacturing, therefore the co-curing of interphase capable materials is selected. A TP/TS combination on the basis of an adhesive interface will provide the reference case in investigating the TP/TS attachments.

The second main challenge is avoiding thermal degradation of the thermoset resin [5, 10]. Fusion bonding requires a temperature above the melt temperature for semi-crystalline thermoplastics and above the glass transition temperature for amorphous thermoplastics in order for the fusion bonding to take place [4]. These high temperatures can induce thermal degradation (loss of physical, mechanical or electrical properties [11]) of the thermoset resin through phase separation because most commercial thermoset resin blends are not in

thermodynamic equilibrium [12]. Higher temperatures can result in polymer decomposition, where the polymer forms gaseous, burnable vapours [11]. It was shown that fusion bonding can induce sublimation of the thermoset resin [5]. The challenge is exemplified by the materials used in this research, discussed in subsection 1.1.3. The M18 thermoset resin is cured at 180°C, it has a maximum operating temperature of 135°C [13] while in close proximity 217°C for PEI and 343°C for PEEK is required for fusion bonding. The issue can be circumvented by choosing a thermoplastic with a low processing temperature [14] or prevented by sufficient heat capacity of the interlayer [15] to shield the thermoset resin. Lastly Villegas et al. [5] proposed a minimal heating time to prevent degradation, using the property that degradation is a time dependent process, if the time is short enough then it can be prevented [16]. Additionally the minimum time minimizes the time for heat diffusion, decreasing the temperature in the thermoset material [5]. The selection of a suitable fusion bonding process for this research is on the basis of preventing thermal degradation. Available fusion bonding techniques for thermoplastics are given in [2, 17, 18]. Resistance welding seems to be the preferential indirect fusion bonding technique for thermoset composites, used by Ageorges et al. [19], Hou [20], Don et al. [10] and McKnight et al. [21]. Discussion on the degradation in this research as well as the bonding between the TS to TP remains limited. In another paper Hou [22] discusses the interphase between a TP with a glass transition temperature below the curing temperature of the co-cured TS, which is not the preferred approach in this research. Villegas et al. [5] used ultrasonic welding to study degradation due to welding and proved that this technique can prevent degradation, attributed to sufficiently short heating times in the order of 500ms. This technique is thus selected for this research because of its proven effectiveness.

1.1.2. Ultrasonic welding

The available fusion bonding techniques can be classified according to their method of heat introduction [2]. Ultrasonic welding locally introduces heat into the joint by generating vibrations normal to the weld overlap, which are inserted into the joint by physical contact with a sonotrode that presses on the joint with a specific force, Figure 1.1. These vibrations compress and decompress the weld overlap, yielding heat that melts (semi-crystalline thermoplastics) or softens (amorphous thermoplastics) the fusible material. An energy director (ED) is used to focus the heat generation, it possesses the least resistance to cyclic straining imposed by the vibrations [23]. The ED compresses and subsequently expands in thickness, simultaneously the ED expands and contracts in the orthogonal directions. The cyclic straining produces heat through viscoelastic friction while interfacial friction between the ED and the parts to be joined produces additional heat [24]. When welding composites flat ED's can be used instead of the legacy triangular ED's as depicted in Figure 1.1. These flat ED's are neat resin films, the preferential heating of the flat ED is maintained because the composite has a higher resistance to the cyclic straining than the neat resin [25]. Villegas et al. showed that it is possible to get consistent, high-quality welds if flat ED's are used in combination with displacement controlled welding [25], where the weld process is terminated after reaching a certain downward travel of the sonotrode while heated ED material is squeezed out of the weld overlap. During welding the welding system provides feedback such as sonotrode travel and dissipated power, which can be related to physical occurrences in the weld overlap. This feedback is used for fast and effective determination of the optimum input parameters for the welding system. Since a consistent process is desired, flat ED's and travel controlled welding are selected for this research. The most important welding parameters for this research are welding amplitude, welding force and sonotrode travel. These three parameters are decisive for the heating time [26], important for preventing thermal degradation of the thermoset material in this research.

In subsection 1.1.1 a strong TS/TP attachment was identified as a main challenge. Previous research by Nicolás Morillas [9] confirms this statement. This research showed that ultrasonic welding can create voids and induce burning of the co-cured layer along the whole weld overlap. This was the case for some surface treated co-cured interlayers. Additionally Nicolás Morillas [9] reports minimal lap shear strength (LSS) values for the joints where the co-cured layer have voids and burning, e.g. 11.91MPa for chloroform and amine treated PEKK film co-cured on a M21 laminate. It is therefore of importance that the post-weld TP/TS connection, the interphase is inspected for any influence from the welding process.

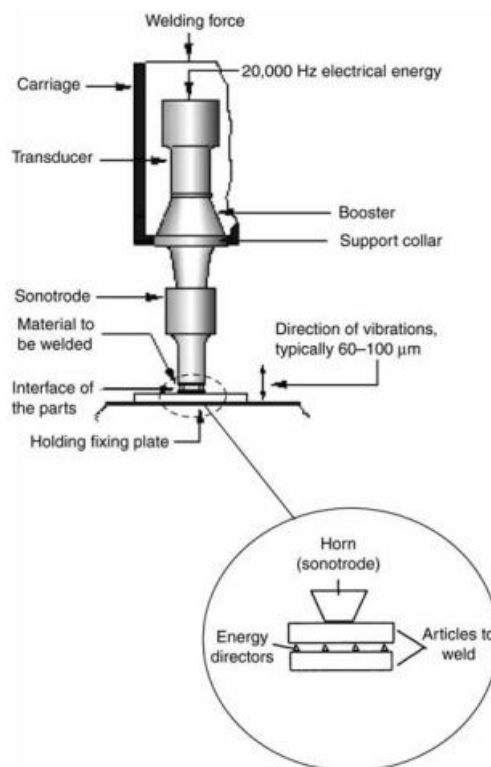


Figure 1.1: Schematic for an ultrasonic welder, figure from [27].

1.1.3. Interphase formation mechanism

Most discussions in literature on planar interphases between a thermoplastic interlayer and a thermoset resin are rather limited in how they were formed. Most interlayers are designed to form an adhesive bond with the thermoset resin during cure [21], defined in this research as an adhesive interface. This type of interlayers probably will have the same certification issues as adhesively bonded joints, briefly discussed in subsection 1.1.1. If an initially soluble material combination is chosen for the interlayer and the thermoset material an interphase may form [28], which is a gradual transition between the two materials. An interphase is a polymer blend with a gradient concentration of the polymers. There is some confusion in literature between semi-interpenetrating networks (s-IPN) and interphases. The authors of papers [10, 22, 29] mention a s-IPN as the mechanism that attaches the two materials to each other. A s-IPN is defined [30] as a linear or branched polymer that is interlaced with a crosslinked polymer, without the presence of a covalent bond. S-IPN are in the order of nanometers [30] while the interphases discussed in this research and literature [22, 28, 29, 31, 32] are in the order of micrometers. S-IPN might be present in the interphase, but not on the size scale discussed here. Lestriez et al [28] pointed out the difference between s-IPN and interphases and discussed in greater detail the forming mechanisms and constraints of an interphase. This research follows this school of thought, detailed here on the basis of the paper from Lestriez et al. [28], a book on polymer blends [33] and a review paper on dissolution processes [34]. A good understanding of the formation process is recommended to understand the morphology obtained and discussed in section 3.2.

During cure the initially soluble materials are in physical contact at a temperature which is typically below the glass transition of the thermoplastic material. The initial solubility implies that the two contacting materials can diffuse into each other, which takes place through dissolution of the glassy thermoplastic polymer. During dissolution the components of the thermoset resin disentangle and dissolve the thermoplastic polymer chains, followed by Fickian diffusion of both materials into each other. The diffusion speed is dependent on the local concentration of and their affinity to the components of the thermoset resin (epoxy and hardeners) and the thermoplastic polymer, as well as their respective molecular structure and van der Waals volume. This process creates a gradient concentration of both materials (or more accurately, the components of the materials). While the dissolution process takes place the molecular weight of the thermoset polymer chains

increases because of the polymerisation of the thermoset resin. The thermoset polymer chains lose their solubility because of the increased weight, whereby they phase-separate from the thermoset-thermoplastic solution, which ceases the diffusion process [28]. Alternatively the diffusion process changes the local concentration of the materials, which can also trigger phase separation. In this research both phase separation mechanisms occur.

As is the case with metals, a phase diagram can be created which can help understand what is happening during cure. In this case a component of the solution is polymerising, which adds an additional dimension to the phase diagram. For example Figure 1.2 shows a theoretical upper critical temperature solution (UCTS) phase diagram for a binary material system where one component experiences polymerisation. The curve, a function of temperature and weight percentage of one of the two materials is called the binodal line. It delimits the single phase region, where diffusion is possible, from the dual phase region, where phase-separation occurs because solubility is lost and hence the diffusion capability. UCTS is associated with phase separation at 'low' temperatures, the binodal line resembles an inverted parabola, with a peak at the top. Lower-CTS also exist, they resemble normal parabolas, they are associated with phase separation at 'high' temperatures. Both curves can be present in one material system. There are also material combinations that are completely soluble or not soluble over the entire temperature and composition range. Focusing on the UCTS curve, the polymerisation moves the UCTS binodal line upwards and to the right as indicated by the arrow in Figure 1.2.

In metals the temperature is decreased to solidify the melt and the phase diagram curves remain fixed, phase separation is initiated by decreasing the temperature. In the case discussed here the temperature remains at the curing temperature, the polymers vitrify as the glass temperature of the local blend increases under influence of the polymerisation, meanwhile the binodal line moves due to the polymerisation as discussed. Phase separation is initiated by crossing the moving binodal line vertically and/or crossing the binodal line horizontally because the local ratio of the different materials changes due to the diffusion of the different components at different diffusion speeds and directions. A property that will be used later in this research is that increased concentrations of thermoplastic can delay phase separation initiated by polymerisation, see Figure 1.3, increasing the time for diffusion [28].

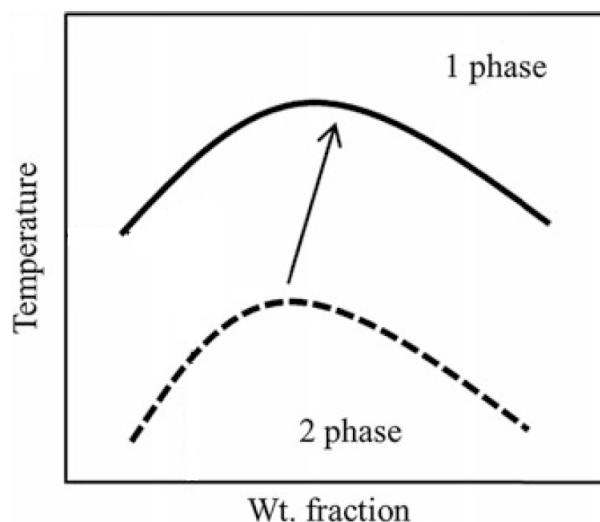


Figure 1.2: UCTS phase diagram of a binary polymer system, during polymerisation of one of the components in a polymer blend the phase diagram shifts as indicated by the arrow. Image adapted from [33].

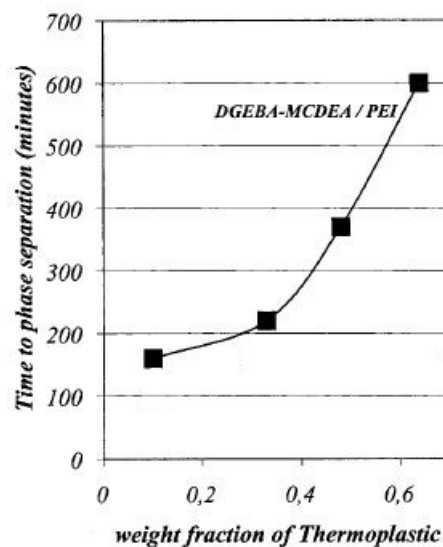


Figure 1.3: Time to phase separation for DGEBA MCDEA PEI mixture during isothermal cure at 135°C for different PEI weight fractions. Image adapted from [28].

The crystal structure of a metal is determined by the local concentration ratio of the different components in the metal. The same is true for vitrifying polymers, they obtain a certain morphology which depends on the local concentration ratio of the different components in the polymer blend. This morphology can also be predicted with a phase diagram as is the case with metals. Figure 1.4 shows an UCTS phase diagram. This time also the spinodal curve is shown. If the phase separation occurs in the region between the binodal and

the spinodal curves then the polymer morphology will be formed by nucleation and growth (NG). This results in a morphology where spheres of one polymer are embedded in a matrix of the other polymer. Otherwise the morphology will form by spinodal decomposition. The peak of the two curves are in the same location, thereby a material ratio at this composition, called the critical composition, will form a morphology by SD only. SD results in a co-continuous morphology. Images of these morphologies are shown later in section 3.2. In this research both mechanisms will be observed because of the concentration gradient present in the interphase.

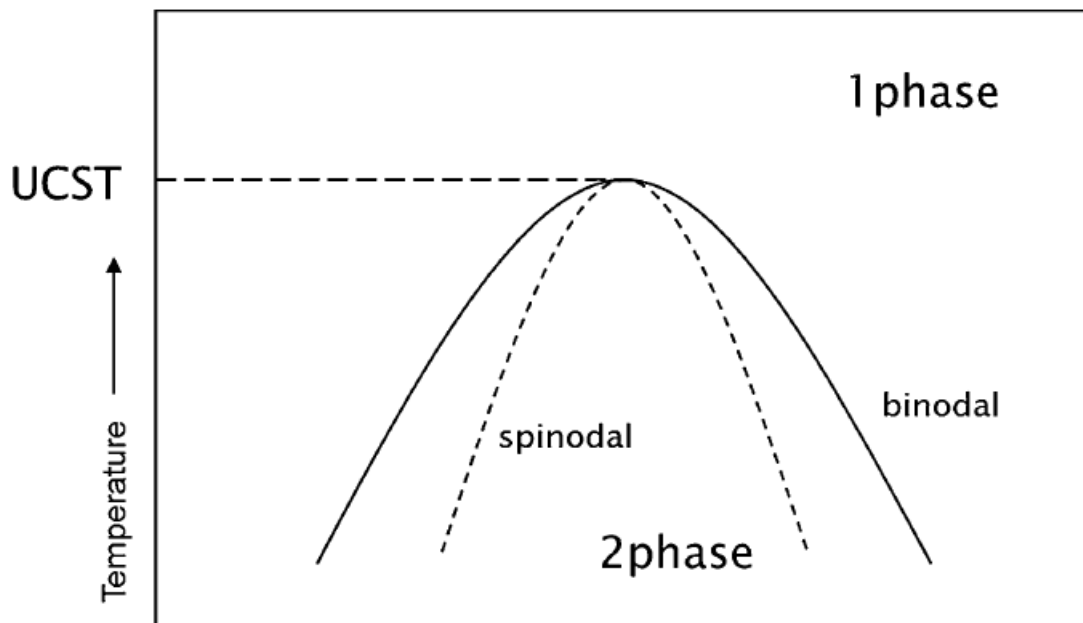


Figure 1.4: UCST phase diagram of a binary polymer system. The full line is the binodal line that delimits the single phase from the dual phase. The dashed line is the spinodal line. Between the binodal line and the spinodal line phase separation occurs through nucleation and growth (NG), outside this region the phase separation occurs by spinodal decomposition (SD). Image adapted from [33].

1.1.4. Interphase evaluation methods

Detailed analysis of the interphase morphology is required to compare the interphase before and after welding. A review of techniques used in literature to inspect the interphase is presented, so that the most suitable techniques for this research can be selected.

Optical microscopy is used by Heitzmann et al. [31], Figure 1.5, and Vandi et al. [29], Figure 1.6. The morphology of the interphase was visible with Vandi et al. [29] but not with Heitzmann et al. [31]. Optical microscopy requires a contrast to see details [35]. Scanning electron microscopy (SEM) uses an electron beam to scan the surface of a specimen. Rajagopalan et al. [32], Figure 1.7, Lestriez et al. [28] and Gilmore et al. [36] use the technique. Etching with a solvent can increase the topographical contrast [28, 32]. Transmission electron microscopy (TEM) uses an electron beam that passes through a thin sample, used by Lestriez et al. [28]. Atomic force microscopy (AFM) is a mechanical technique that uses a vibrating cantilever to probe the surface. So called phase images relate the image to the type of material under the probe. Topographic images display the surface topography. AFM is used by Vandi et al. [29], Figure 1.8 and Hou [22].

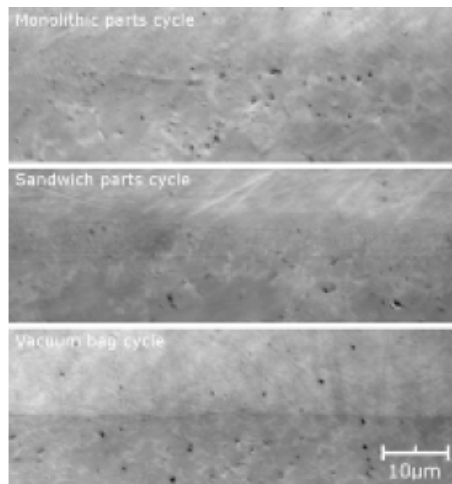


Figure 1.5: Optical microscopy image of co-cured M18 resin from Hexcel with PEI for different cure cycles. Image from [31].

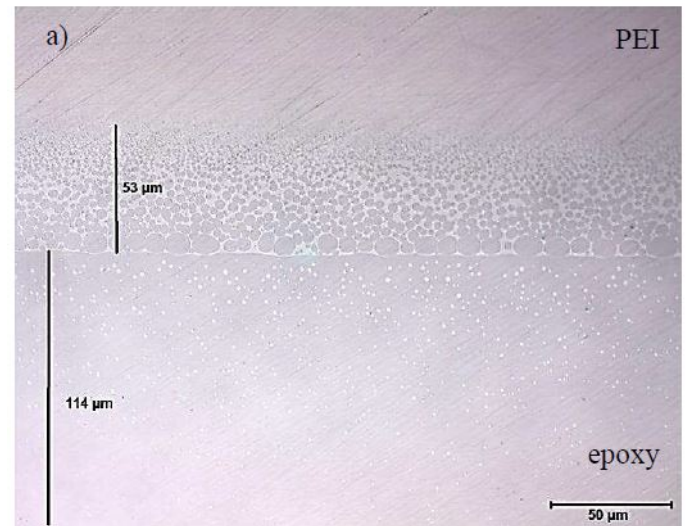


Figure 1.6: Optical microscopy image of epoxy (tetraglycidyl diaminodiphenyl methane (TGDDM), diglycidyl ether of bisphenol F and triglycidyl-p-aminophenol with diaminodiphenyl sulphone (DDS) hardener) co-cured with PEI. Image from [29].

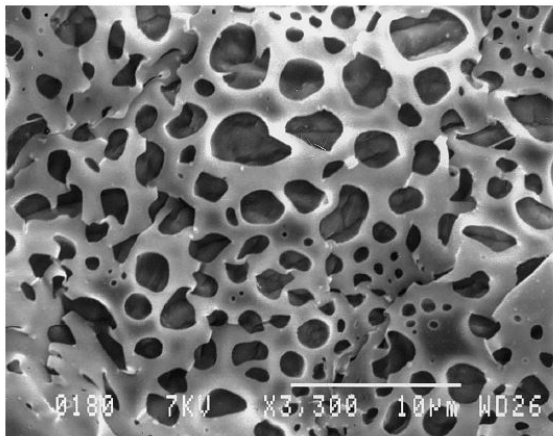


Figure 1.7: SEM image of co-cured epoxy (diglycidyl ether of bisphenol A (DGEBA) with bis-cyclo hexyl diamino methane (PACM 20) hardener) co-cured with PSU, the PSU has been etched away. Image from [32].



Figure 1.8: AFM phase image of epoxy (tetraglycidyl diaminodiphenyl methane (TGDDM), diglycidyl ether of bisphenol F and triglycidyl-p-aminophenol with diaminodiphenyl sulphone (DDS) hardener) co-cured with PEI. Image from [29].

1.1.5. Material selection

The long-term goal in the research area where this thesis contributes is to weld a CFPEEK bracket to a CF/TS skin for aerospace applications. This thesis will use a co-cured interlayer and ultrasonic welding to work towards this goal. Therefore initially soluble aerospace grade materials need to be found. A proven material combination is desirable because it is not the aim to research interphases or interphase formation. With these constraints only one published research paper was available by Heitzmann et al. [31]. This paper discusses the interphase between a Ultem 1000 PEI film from SABIC co-cured with carbon reinforced M18/1 (CFM18) thermoset resin from Hexcel. The paper provides only limited amount of experimental evidence for the interphase, but solubility requirements are assured since the thermoset resin already contains Ultem 1000 PEI as a toughening material [31]. The ability to weld PEI films with CFPEEK is already proven in previous research by Nicolás Morillas [9]. Moreover Crevecoer et al. [37] proved that PEI and PEEK are completely miscible over the entire range of mixing ratios when PEEK is amorphous. Since welding requires the melting temperature for the semi-crystalline PEEK, the molten state ensures that PEEK is amorphous and therefore miscible during welding, hence a fusion bond can be created. CFM18 from Hexcel is therefore selected as substitute for the CF/TS skin, a PEI co-cured film will be used as interlayer, since this material combination is likely to form an interphase. The thermoset laminate with the interlayer will be welded to a CF/PEEK laminate, Cete TC1200 from Tencate. The reference adhesive interface will use the same CFM18 and CFPEEK laminate. But this time a PEEK film will be used as the co-cured interlayer. Experimental results from this research showed that PEEK is incompatible with M18, because it is unable to adhere to the laminate after cure if no surface treatments are performed on the PEEK. Surface treatment will allow the PEEK film to remain adhered.

1.1.6. The manufacturing environment

Introducing amorphous PEI into the joint raises questions on the performance of the joint when exposed to moisture and solvents, since amorphous PEI is more susceptible than e.g. the semi-crystalline PEEK. Furthermore previous unpublished experience from research of Vizcaino Rubio [8] raised questions on the integrity of joints with surface treated films when these are exposed to a humid environment. The joints will be created with ultrasonic welding, a fusion bonding process. Literature indicates that fusion bonded joints require less surface preparation than adhesively bonded joints [2]. This implies that fusion bonded joints should be less sensitive to surface contaminants. These observations can be themed as a manufacturing environment in a commercial production process. The joints are exposed to moisture during C-scan inspection, cleaning solvents are used and there is a probability of contaminants on the surface. The welded joints that are created in this research are therefore also exposed to moisture and a solvent, as well as a contaminant before welding, the performance of these joints is then compared to non-treated joints.

1.2. Research questions and objectives

This thesis builds further upon the research of Pablo Vizcaino Rubio [8] and Maria de Nicolás Morillas [9] on ultrasonic welding with thermoset materials. The work of this thesis is focused on two main topics. Firstly it investigates the connection between the thermoset material and a co-cured thermoplastic interlayer, which provides a fusible layer. Then the thesis proceeds with evaluating the strength of the joints created with ultrasonic welding, using this interlayer. Lastly it investigates the performance of these joints when exposed to the manufacturing environment.

The long-term goal in the research area whereto this thesis contributes is to weld a CF PEEK bracket to a CF TS skin for aerospace applications. This thesis works towards this goal by investigating the possibility to use an initially miscible, co-cured interlayer as fusible surface. In this way the certification issues associated with adhesive bonding can potentially be circumvented.

The thesis objective is to investigate if the connection is affected by the welding process and if the created joints last when exposed to the manufacturing environment. To meet this objective the research is divided into two activities. The first activity is to study the interphase before and after welding, comparing presence, morphology and size. In the second activity the performance of the joints in a manufacturing environment is tested and compared on the basis of their lap shear strength and fracture surface.

The thesis will form an answer to the following research questions:

- Can the interphase between the interlayer and the thermoset material be observed with the equipment available within the TU Delft?
- Is the interphase affected by the welding process?
- How strong are the welded joints created with this interlayer approach?
- Are the joints highly sensitive to the production environment?

Carbon fibre embedded in M18/1 (CFM18) resin from Hexcel is used as a thermoset laminate, this will be co-cured with a PEI Ultem 1000 co-cured interlayer from SABIC as fusible interlayer. This material combination is expected to form an interphase. The thermoset laminate with the interlayer will be welded by ultrasonic welding to carbon fibre reinforced PEEK (CFPEEK) laminate, using Cetex TC1200 from Tencate. As a reference case a surface treated Vitrex PEEK interlayer is co-cured with CFM18, which is expected to form an adhesive interface to the CFM18 laminate. The available laminates are welded in the following configurations:

- CFPEEK/PEEK/CFPEEK
- CFPEEK/PEI/CFPEEK
- CFM18PEI/PEI/CFPEEK
- CFM18/PEI/CFM18 cured reference joint
- CFM18PEEK/PEEK/CFPEEK
- CFM18PEI/PEI/CFM18PEI
- CFM18PEEK/PEEK/CFM18PEEK

With X/Y/Z as in Figure 1.9.

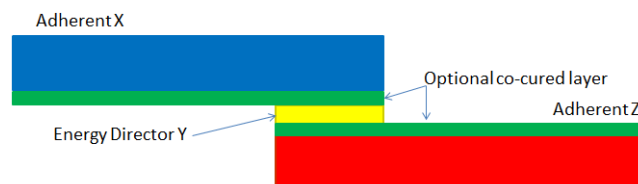


Figure 1.9: Joint anatomy X/Y/Z.

After this introductory chapter there is a brief chapter that details the materials and procedures used during the research. this is followed by the two main chapters. Chapter 3 focusses on the interphase. Interphase assessment techniques are evaluated, then the interphase is inspected, followed by inspection of the post-weld interphase. Chapter 4 discusses joints created by ultrasonic welding, using the co-cured interlayer technique as fusible layer for the thermoset laminate. The optimum welding parameters are established and the joint

configurations detailed previously are manufactured.

The performance of the joints is evaluated as manufactured, at in dry/RT conditions. Followed by exposure to a manufacturing environment, immersion in water as an analogue to C-scan inspection, immersion in the solvent Methyl ethyl ketone (MEK) as analogue to MEK cleaning and a contamination before welding sensitivity test. Finally the conclusions of this thesis are presented in chapter 5, followed by recommendations for future research in chapter 6.

2

Experimental

2.1. Materials

This section details the most important materials used during the thesis. Carbon fibre reinforced materials are used for creating adherends while unreinforced materials are used as energy director during the ultrasonic welding process and optionally as a co-cured film, called the interlayer, where the neat resin is cured while in contact with a thermoset laminate.

2.1.1. Polyether ether ketone

Polyether ether ketone, abbreviated as PEEK is a semi-crystalline thermoplastic polymer. The chemical structure is depicted in Figure 2.1. PEEK has a Tg of 143°C and a melting temperature of 343°C [38]. PEEK can perform in high temperatures, it is flame retardant and has a high resistance to chemicals and solvents. A few examples where PEEK materials are used in aerospace are the Lockheed Martin F-22 access covers and weapon bay doors, Lockheed Martin F-117 rudder assembly and Airbus A320 vertical stabilizer brackets [39].

PEEK films with a thickness of 50µm and 250µm are used. These films are manufactured by Vitrex, grade 1000-050G and 1000-250G. Inhouse DSC measurements indicate an onset of the glass transition at 139°C and ending at 163°C. Also carbon fibre reinforced PEEK is used, which is supplied in sheet form by Tencate under the name Cetex TC1200, a 5 harness satin weave. This material is referred to as CFPEEK. Onset of the glass transition was measured at 123 °C and ending at 200 °C.

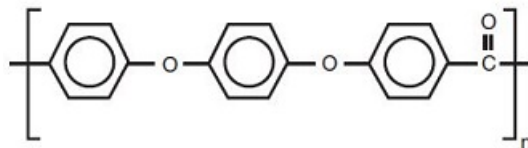


Figure 2.1: Chemical structure of PEEK [39].

2.1.2. Polyetherimide

Polyetherimide, abbreviated as PEI is an amorphous, transparent thermoplastic polymer. The chemical structure is depicted in Figure 2.2. According to the manufacturer it has a glass transition temperature of 217 °C. PEI has a high heat resistance, high strength and modulus and a broad chemical resistance even at high temperature. A few examples where the materials are used in aerospace are Airbus A330-340 lower wing fairings, Airbus 747 stowage bins, Airbus A320 floor panels and brackets in the Boeing 767 [39].

PEI films with a thickness of 50µm and 250µm are used. These films are manufactured by SABIC, under the product name Ultem 1000. Inhouse DSC measurements indicated the onset of the glass transition at 215.8°C and ending at 233.7°C.

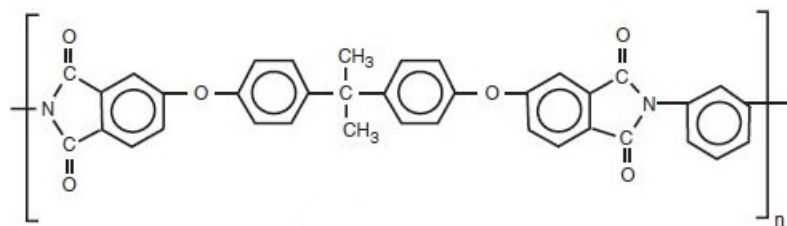


Figure 2.2: Chemical structure of PEI [39].

2.1.3. Carbon reinforced Hexply M18/1

Hexply M18/1 is an epoxy resin system from Hexcel for primary aerospace structures. The resin system is reported to contain tetraglycidyl ether methane diphenyl aniline (TGMDA) with three curing agents: 4,4-Methylenbis-(2,6-diethylanilin) (MBDA), 4,4-Methylenbis-(2-isopropyl-6-methylanilin) (MBIMA) and 4,4-Diaminodiphenylsulfone (DDS) [31]. This resin system is used in the creation of carbon fibre prepreg.

For this thesis the Hexply M18/1 43% G939 is used. Which is M18/1 resin reinforced with carbon fibre 1/4 twill weave. In this thesis the material is referred to as CFM18.

2.2. Manufacturing

This section will detail the manufacturing equipment and outline the procedures used. Unless otherwise mentioned the equipment is from the TU Delft, The Netherlands in the Aerospace Structures & Materials laboratory.

The plies of CFPEEK and CFM18 composite material and neat resin PEI or PEEK films are cut to size with a dragger knife gantry from Gerber and stacked in a symmetric lay-up. CFPEEK laminates consists of 6 plies while the CFM18 laminates have 8 in order to have a final thickness close to 2mm. The thermoplastic laminates are fixed to each other with a manual ultrasonic welder and transferred to a heated press for consolidation. The thermoset laminate is vacuum debulked every 4 plies. The PEI or PEEK co-cured layer is added to the thermoset laminate as the last ply. The side of the PEEK film which is in contact with the thermoset laminate during cure is UV-ozone treated for 30 minutes before lay-up on the laminate, the distance from the UV lamps is 5cm, the PEI film is used as is. Finally the thermoset laminate is transferred to the autoclave.

The Joost heated press and Scholz autoclave are programmed to execute the manufacturer recommended consolidation/cure cycle. Consolidation is at 385°C at 10 bar for 20 minutes. The cure cycle is depicted at Figure 2.3. The bagging system for the cure cycle uses a caul plate to ensure a smooth surface finish on both sides of the laminate.

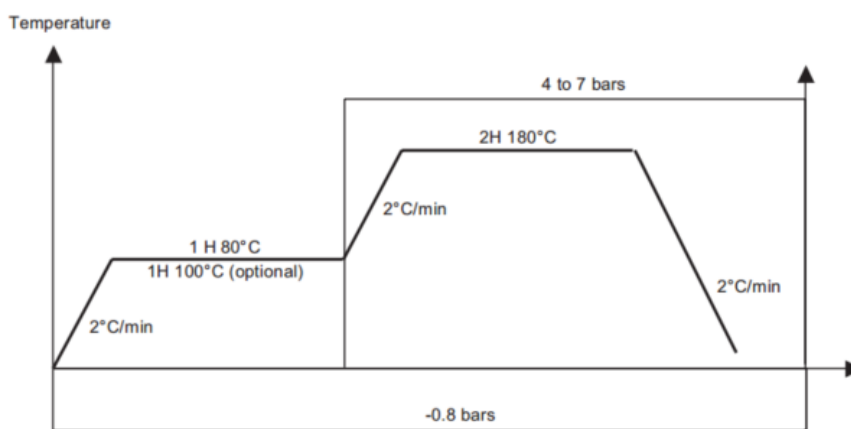


Figure 2.3: Recommended cure cycle for the M18 material, from [13]. In the first phase 90°C is chosen and 7 bar absolute pressure for the second phase of the cure cycle.

After curing/consolidation the laminates are cut into adherends of 25.4x101.6mm with a waterjet at the company Van Nobelen in Delft. Flat energy directors, a bit bigger than the joint overlap are cut from 250 μ m thick neat resin sheets. The PEI containing materials are dried in a vacuum oven and stored in a desiccator. Before welding the adherends and energy directors are cleaned with a degreaser and wiped dry. The adherends are welded to each other with the energy director using optimum welding parameters, using the Rinco Dynamic 3000 ultrasonic welder. It operates at 20Khz and has a power of 3000W, the cylindrical horn with 40mm diameter is used. The selection procedure for these optimum parameters are described in section 4.1.

2.3. Conditioning

Samples require conditioning in water at elevated temperatures for subsection 4.4.1. The samples are placed in a container with purified water at 70°C, see Figure 2.4 and Figure 2.5. The samples are hung in the water by a clamp so that the samples do not touch each other or the container. The container has a lid to minimize water evaporation and a sensor in order to automatically regulate the water temperature. Water evaporation is compensated by adding water of 70°C when the water line approaches the top of the samples. The samples are immersed in room temperature purified water for transfer from conditioning to the tension bench.

Samples require conditioning in MEK for subsection 4.4.2. Samples are placed in a measuring glass cylinder, Figure 2.6. The samples are kept immersed until testing in the testing bench.

The conditioning for the contaminant test is described in subsection 4.4.3.



Figure 2.4: Water immersion container with immersed samples.



Figure 2.5: Water immersion container with automatic temperature control.



Figure 2.6: MEK immersion cylinder with immersed samples.

2.4. Evaluation methods

This section details the equipment used to obtain experimental observations and data.

2.4.1. Microscopy and vibrational spectroscopy

Sample cross sections are prepared for optical microscopy by embedding followed by polishing up to a grit size of $1\mu\text{m}$. Some samples are etched in order to create contrast or partially dissolve PEI. These samples are etched with NMP by dripping 1ml of NMP solvent along the embedded and polished sample. The samples are then rinsed with ethanol and distilled water, followed by drying by compressed air. Two optical microscopes are used, a Zeiss Axiovert 40 and the Keyence VHX-2000 Digital Microscope.

A scanning electron microscope (SEM) is used when larger magnifications than optical microscopy are required. SEM uses an electron beam to irradiate the sample surface. The electrons interact with the sample and are picked up by a detector and processed into an image. Sample conductivity is required so the non-conductive samples are sputtered with a layer of gold. Sample cross sections are prepared in the same manner as for optical microscopy, but with an additional layer of sputtered gold. Fracture surface samples require no preparation except for the sputtering of a gold layer. The JEOL JSM-7500F SEM is used.

Atomic force microscopy (AFM) measures the interaction of a small cantilever with the surface of the sample. The cantilever deflects under the attractive and repulsive forces between the tip of the cantilever and the sample. The deflection is measured by a laser, these measurements yields a 3 dimensional plot of the sample surface. Sample preparation is equal to the optical microscopy, but without the etching. The AFM used is the Nanosurf Nanite B from the Faculty of Mechanical, Maritime and Materials Engineering at the TU Delft, utilised in tapping mode.

Raman spectroscopy uses a laser to irradiate a sample. The laser light is scattered, of which a small portion is scattered inelastically, called Raman scattering. The inelastically scattered light has a different frequency than the frequency of the original light of the laser. The Raman scattering is a result of the laser light interacting with the molecules of the sample, it yields feedback that can be associated with the molecules in the sample. Therefore if an interphase is examined we expect the material associated feedback to shift gradually from the feedback of one material to the feedback of the other material. While an interface should produce a feedback with sudden transition from one material to the other. The Raman spectrum for PEI, PEEK and M18 are plotted in Figure 2.7. In the report the intensity of the 1005cm^{-1} peak is used for generating a false colour plot. The graph shows that PEI has a high response at 1005cm^{-1} , while M18 has a modest response. At the settings used for the Raman spectroscope PEEK only displays noise. This technique is suited to identify the presence of an interphase or interface and it can provide an overview of the shape of the interphase. Sample preparation is equal to optical microscopy but no etching is required. A Renishaw inVia Raman microscope is used during this thesis which uses a 785nm laser. 1% power of the 200 mW laser is used, which irradiates the sample for 1 second per measurement.

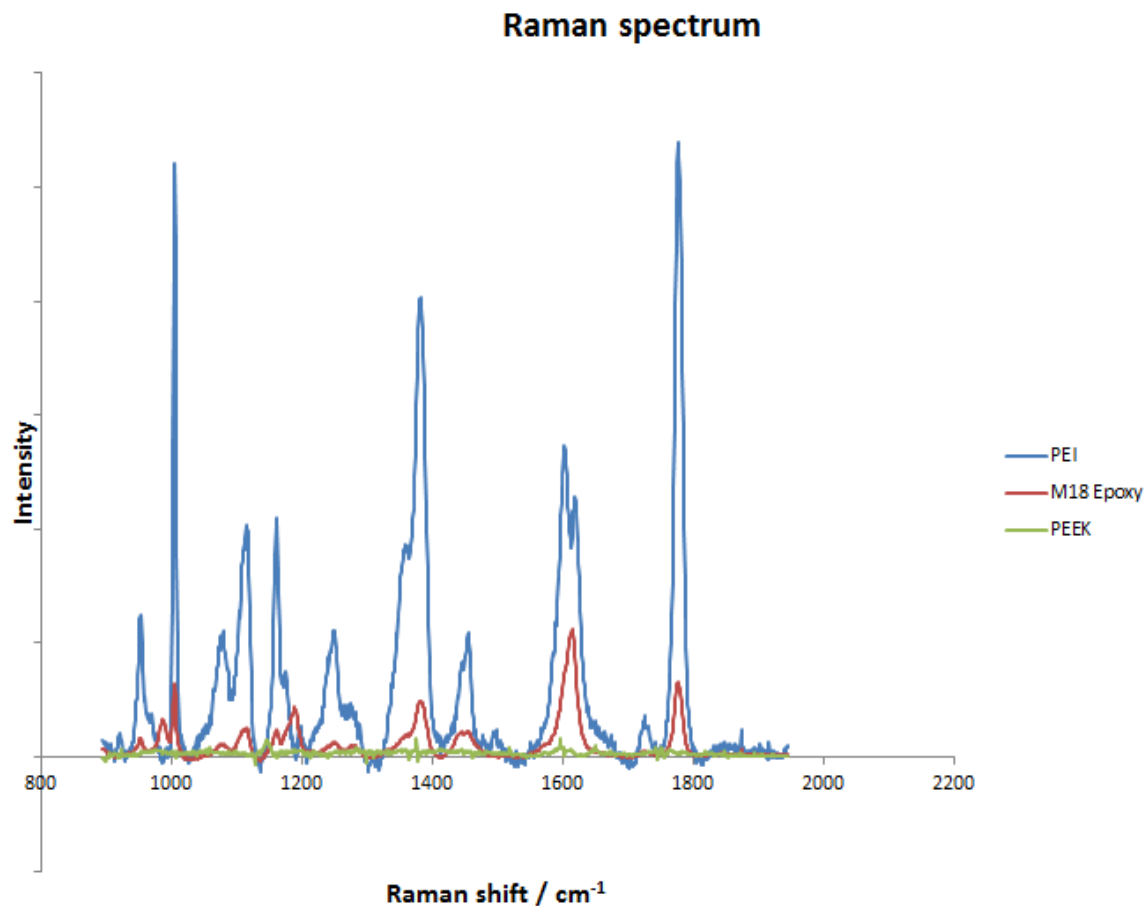


Figure 2.7: Raman spectrum of PEI, M18 and PEEK

2.4.2. Physical testing

Contact angle measurements (CAM) were used to measure the efficacy of the UV-ozone treatment on the PEEK co-cured films. It can measure the wetting properties of a surface and the surface energy [6], properties related to adhesion. The CAM200 from KSV NIMA was used with 3 μ l distilled water droplets.

Differential scanning calorimetry (DSC) was performed to measure the glass transition temperature and melting temperature of the thermoplastic materials. The Pyris Diamond TG/DTA Thermogravimetric/Differential Thermal Analyzer was used in all measurements with a heating rate of 20°C/min.

2.4.3. Mechanical testing

The welded joints are tested according to ASTM D1002, with 5 samples per test. The adherends of the joints are 101.6x25.4 mm, with a weld overlap of 12.7 mm. The tension bench was the Zwick 250 KN with the crosshead speed set to 0.13 mm/min, vertical distance between the clamps is 60cm, the clamps are off-set to align the load with the weld overlap. The apparent single-lap shear strength (LSS) of the joint is obtained by dividing the maximum load by area of the weld overlap. The type of fracture is also analysed.

II

Experiments, results & discussion

3

Investigations in weldable thermoset materials

3.1. Interphase assessment techniques

This chapter concentrates on the inspection of interphases between the 3 selected materials, CFM18, PEI and CFPEEK. CFM18 co-cured with PEI is expected to form an interphase between each other while CFM18 co-cured with PEEK is expected not to form an interphase. First suitable interphase assessment techniques need to be established. Techniques reported in literature for the study of TP/TS interphases are optical microscopy [29, 31], Scanning electron microscopy (SEM) [28, 32], Transmission electron microscopy (TEM) [28], Energy dispersive X-ray (EDX) [31] and Atomic force microscopy (AFM) [22, 28, 29]. Some of these techniques, optical microscopy, SEM, TEM and AFM are evaluated for their suitability in this research. An additional technique that was used in this research is RAMAN spectroscopy, explained in subsection 2.4.1 and subsection 3.1.2. EDX could not be used in this research because of the absence of a suitable tracer element in the materials used in this research.

3.1.1. Microscopy analysis

Optical microscopy of as-polished cross sections of CFM18PEI and CFM18PEEK reveal that there is a colour contrast between CFM18 and PEEK, Figure 3.1. None or limited colour contrast is available between CFM18 and PEI, depending on the lighting settings and the microscope, Figure 3.2. Literature [28] prescribes etching to generate contrast between two different materials. Several solvents were investigated for etching samples: N-methyl-2-pyrrolidone (NMP), dimethylacetamide (DMAC), dimethylformamide (DMF) and Ethylacetat. Among these, NMP was selected because it has a satisfactory dissolving potency. Ethylacetat was too weak as a solvent, on the other hand DMAC and DMF were too potent, during etching they dissolved the embedding resin more aggressively, causing embedding resin to cover the sample. The Figure 3.3 shows that a colour contrast is generated after etching of the CFM18PEI sample. The optical microscope allows for easy identification of the co-cured layer. But the resolution is too small for identifying the presence of an interphase.

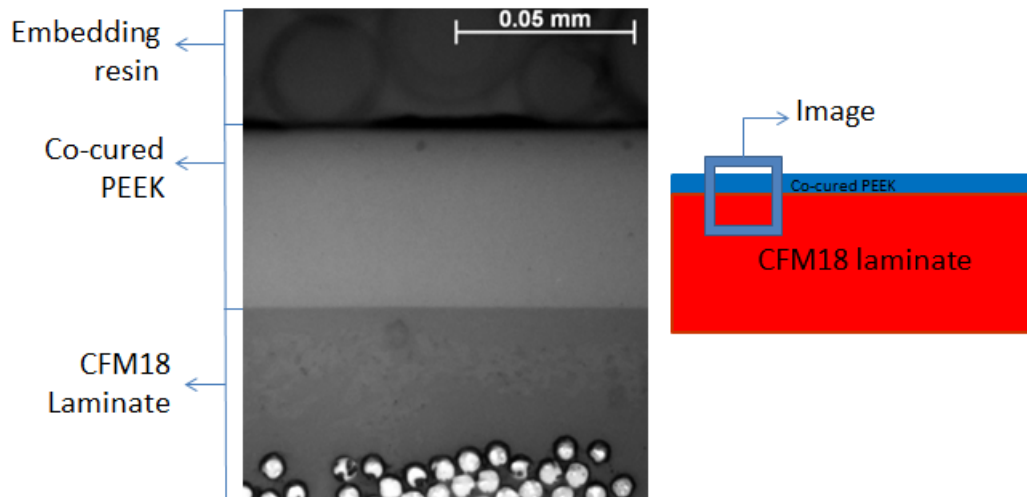


Figure 3.1: Optical microscopy image of a CFM18 laminate with a co-cured 50 μm PEEK film. The co-cured PEEK film has a colour contrast with CFM18.

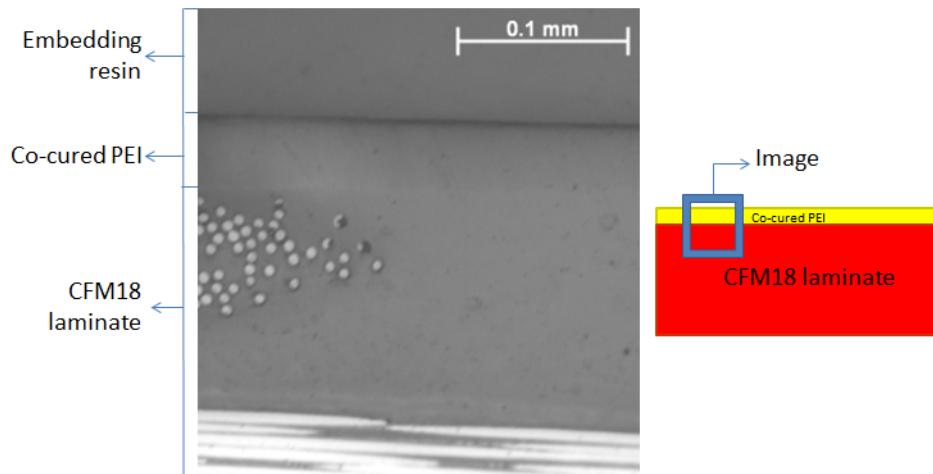


Figure 3.2: Optical microscopy image of a CFM18 laminate with a co-cured 50 μm PEI film. The co-cured PEI film has limited colour contrast with CFM18. Note that in this sample the embedding resin is different then in Figure 3.1.

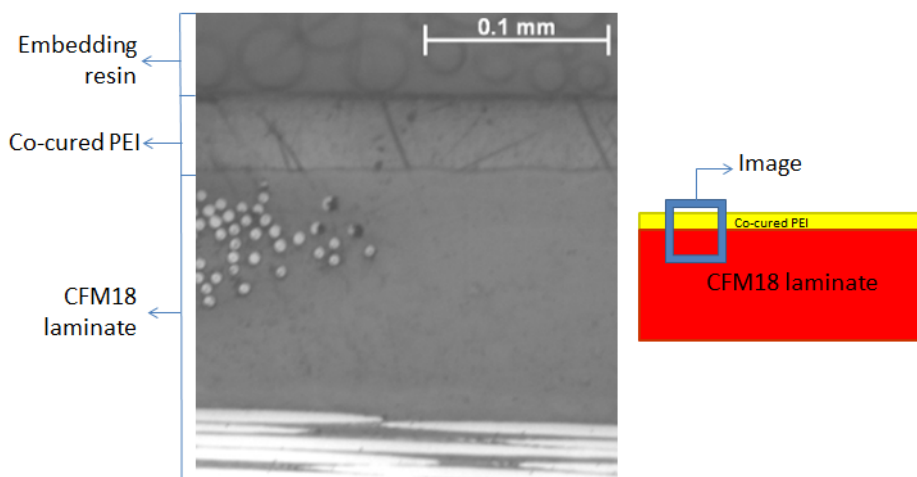


Figure 3.3: Optical microscopy image of a CFM18 laminate with a co-cured 50 μm PEI film. The sample is etched with NMP, the contrast between the CFM18 and PEI increases. Also polishing scratches in the PEI become visible and the embedding resin is affected as well.

Figure 3.1 shows that the PEEK film adheres to the CFM18 laminate after UV-ozone treatment, the image shows that there are no gaps between the two materials. When untreated PEEK was co-cured with the CFM18 laminate the PEEK film detached from the laminate right after cure. Therefore during cure there was no diffusion between PEEK and CFM18, which would result in the materials being attached to each other, neither did the interface between the two materials develop sufficient adhesive strength. The UV-ozone treatment cleans the sample through decomposing organic contaminants [40] and increasing the surface oxygen concentration, thereby increasing wettability and the surface energy [41]. This results in better adhesive properties at the surface of the material. The UV-ozone treatment described in section 2.2 reduced the water contact angle on the PEEK surface from 80.2° to 29.9° . The PEEK film now forms an adhesive interface with the M18 resin.

Figure 3.3 shows that the untreated PEI film attached to the M18 resin after cure, there are no gaps between the materials. SEM allows for larger magnifications than optical microscopy. Unmodified samples do not reveal their morphology under the SEM, see Figure 3.4. Heitzmann et al. [31] reports that M18 contains 20 wt% of PEI. Therefore the etching technique can be used to dissolve a superficial layer of PEI within the M18 resin. In this way the morphology of the M18 resin, potentially diffused into the co-cured layer is made visible at the magnifications offered by SEM, demonstrated by Figure 3.4. This allows for identification and inspection of the interphase, discussed in section 3.2.

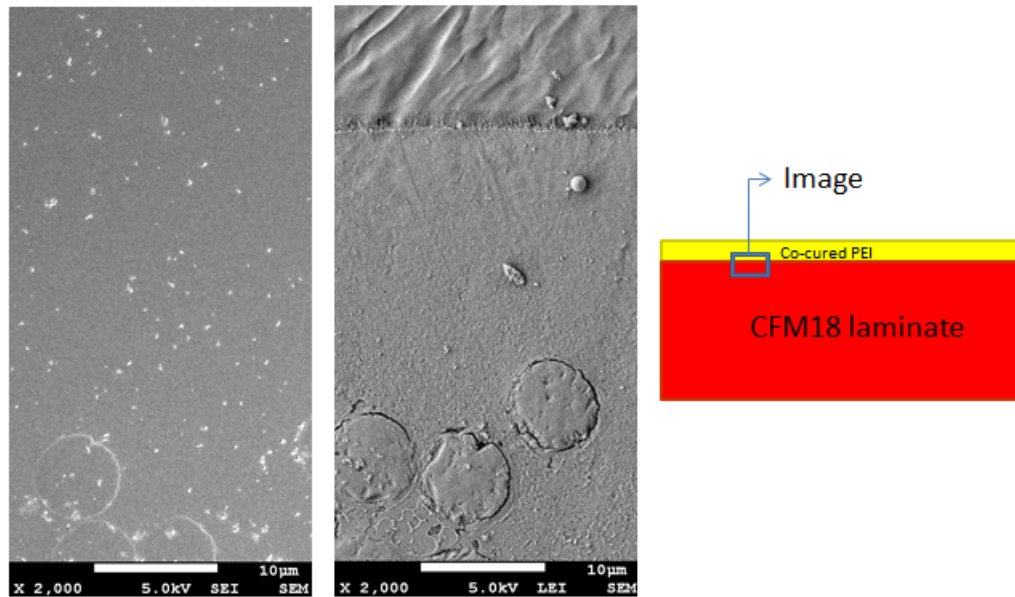


Figure 3.4: Figure on the left: SEM image CFM18 with PEI laminate without etching; Figure on the right: SEM image CFM18 with PEI after etching.

3.1.2. Raman spectroscopy

RAMAN spectroscopy can be used to determine the local concentration of a material. This concentration gradient is in relation to the presence of an interphase between two polymers, since the interphase is a gradual transition between the materials. It is not possible to inspect morphology with this technique. The advantage of Raman over SEM with etched samples is that the interphase can be inspected at a magnifications similar to optical microscopy. It shows a false colour plot of the local material concentration with a resolution of about $1\mu\text{m}$. Figure 3.5 shows the presence of such a gradient in a polished CFM18PEI sample. Figure 3.6 confirms the inexistence of any concentration gradients in a CFM18PEEK sample within the resolution of the Raman spectroscopy, as expected.

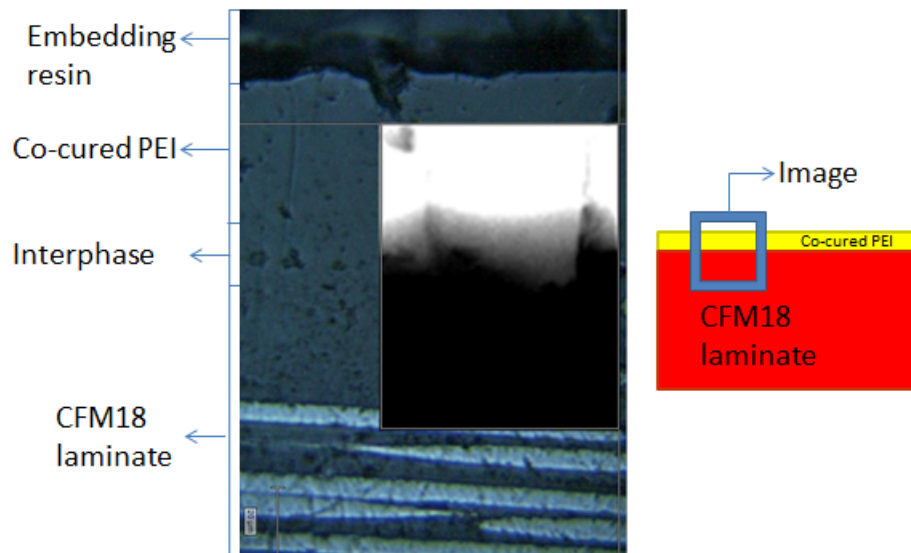


Figure 3.5: Raman false colour image of CFM18 with a PEI co-cured film, showing the intensity of the 1005 cm^{-1} peak. Peaks corresponding to carbon fibre and epoxy are displayed black. Peaks corresponding to PEI are indicated white. The image indicates the presence of an interphase.

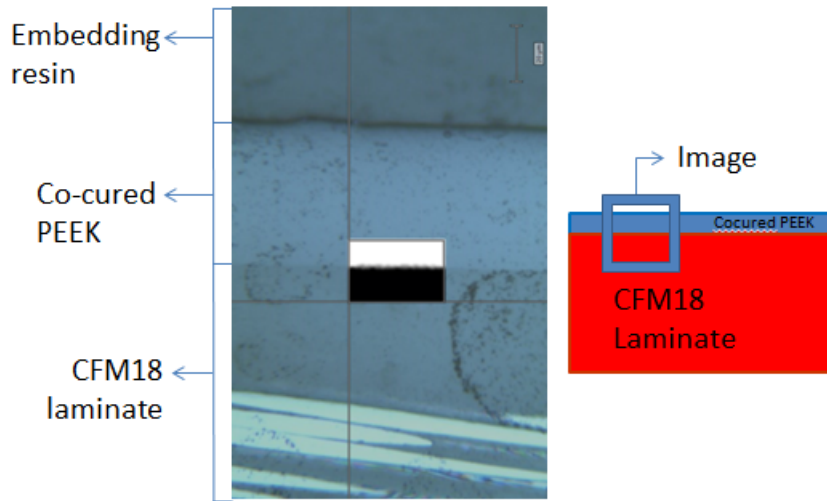


Figure 3.6: Raman false colour image of CFM18 with a PEEK co-cured film, showing the intensity of the 1005 cm^{-1} peak. White indicates pure PEEK while black indicates pure epoxy. The image indicates that there is no interphase.

3.1.3. Other techniques

AFM results are not usable to draw any conclusions because the measurements have too much noise and too low resolution. Furthermore the navigation on the sample is very cumbersome. All this is attributed to the AFM apparatus which is basic, the Nanite B AFM from Nanosurf located at the Mechanical, Maritime and Materials Engineering faculty at the TU Delft. The inability to use the results from this AFM is illustrated by Figure 3.7, which displays a groove as indicated in the figure. This groove could either be the gap between the embedding resin and the sample or the epoxy flow front, discussed later in subsection 3.2.3. Since it was not possible to even identify such a feature with certainty it is not possible to draw any conclusions or make observations from the image.

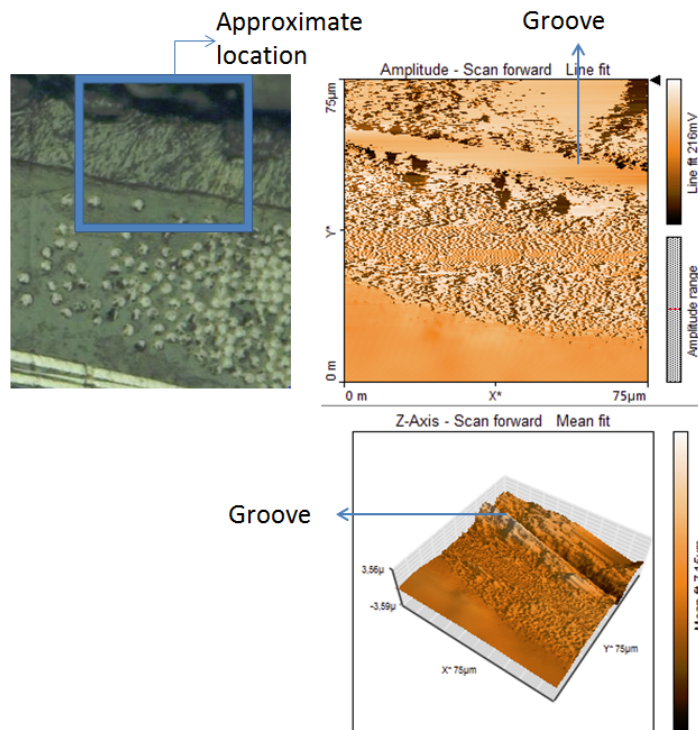


Figure 3.7: AFM image of a CFM18 laminate with a co-cured $50\ \mu\text{m}$ PEI film.

TEM was also considered as a measurement technique. TEM samples need to be very thin so that they are electron transparent [42]. Creating thin slices of the samples by microtoming was unsuccessfully attempted. The sample became a powder instead of thin slice.

3.1.4. Conclusion

From the tried techniques, optical microscopy, SEM and Raman spectroscopy are selected. Of these techniques, SEM in combination with etching is the most powerful. This technique will be used for evaluating the morphology of the M18 resin with their co-cured layer. It will yield results on the interphase morphology, the interphase size, the influence of welding and where joints break. However SEM is not capable to provide an overview to the researcher due to the high magnifications. Raman and optical microscopy will provide a better overview. For example optical microscopy can provide a general overview of where joints break and can thus be used in conjunction with SEM when the fracture approaches the interphase zone.

3.2. Morphology of the interphase

3.2.1. Morphology of the M18 resin

M18 is an epoxy system toughened with 20 wt% PEI. The epoxy system contains the epoxy TGMDA and 3 curing agents, MBDA, MBIMA and DDS [31]. As explained in subsection 3.1.1 the sample needs to be etched in order to reveal morphology. SEM inspection of an etched M18 sample shows the same morphology as observed in the research of Lestriez et al. [28], displaying co-continuous morphology, Figure 3.8, formed by spinodal decomposition (SD), typical of a toughened epoxy system where the toughening thermoplastic is at a critical ratio to the epoxy system [28]. It could be that the M18 morphology is not purely formed by spinodal composition, but that the morphology was briefly formed by nucleation and growth (NG) and then transitioned to the SD mechanism. This is possible because of the moving binodal and spinodal lines during cure. Morphology formed by NG and SD would explain the small circles (typical for NG) inside the morphology formed by SD seen in the figures of Figure 3.8. Lestriez et al. notes in their example that the morphology observed in his image, repeated in Figure 3.8 is formed at the critical composition where only SD takes place. That the M18 resin is formed by pure SD or a combination of SD and NG is not of importance for answering the research questions in this research, therefore pure SD formation is assumed. If a layer of TP which is initially miscible with M18 (such as PEI) is co-cured while in contact with the M18 thermoset resin there will be some diffusion of the thermoset resin in the TP and viceversa which will locally affect the ratio of PEI/thermoset resin, this changes the morphology formation from SD to NG, or a combination of SD and NG because of the moving binodal and spinodal line during polymerisation.

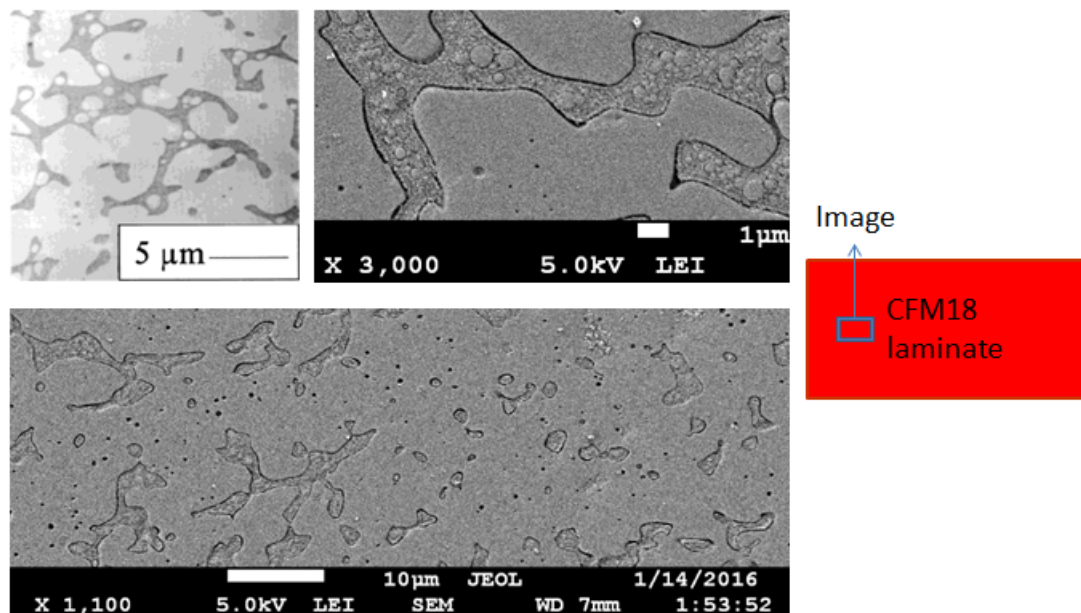


Figure 3.8: Image in upper left corner, co-continuous morphology of DGEBA-MCDEA epoxy blended with PEI at the critical composition, from Lestriez et al. [28]. Lower image and top right image, cross section SEM image of the M18 resin etched with NMP at different magnifications. It also displays the co-continuous morphology.

3.2.2. Morphology of M18/PEEK interface

Figure 3.9 shows that the M18 morphology is maintained in the presence of a co-cured UV-ozone treated PEEK layer. The morphology was not altered, therefore mutual interdiffusion of the chemical constituents of the M18 resin with the PEEK material did not occur, this confirms the lack of miscibility between PEEK and M18, explained in subsection 3.1.1.

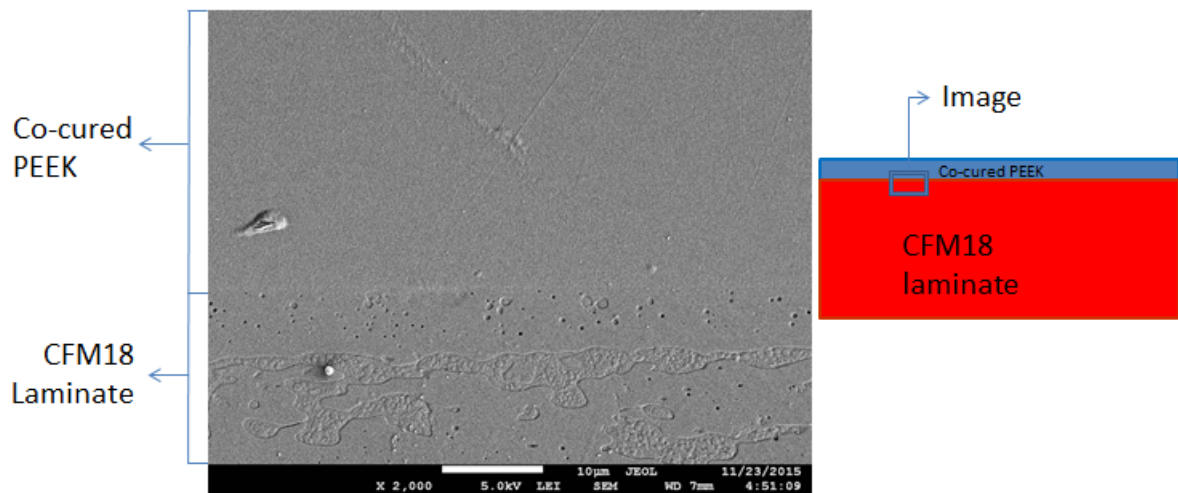


Figure 3.9: SEM image of the interface between the M18 and a co-cured PEEK film.

3.2.3. Morphology of M18/PEI interface

Figure 3.10 shows that the morphology of the M18 resin is altered, it shows the different morphologies that can be found in the M18/PEI samples resulting from the interdiffusion of the PEI and M18 polymers through their interface. Figure 3.11 are higher magnifications of the specific morphologies. Six different zones can be distinguished in the M18/PEI cross section: (1) pure M18, with M18 morphology; (2) M18 with increased PEI content resulting from diffusion of epoxy into PEI and viceversa, characterised by dispersed epoxy spheres in PEI matrix, typical for morphology formed by NG. The size of the epoxy spheres decreases as the PEI content increases, clearly visible in the centre figure of Figure 3.11; (3) PEI with only a limited amount of epoxy, characterised by having only very small epoxy domains and similar response as PEI to etching, resulting in micro-cracks, Figure 3.12 and polishing, resulting in scratches, Figure 3.13. These two responses happen within the top $50\mu\text{m}$ of the sample, which corresponds to the thickness of the original co-cured layer; (4) epoxy diffusion front, with an increased concentration in epoxy that makes the epoxy spheres locally bigger; (5) darker band that could be the result from faster diffusion of hardener into PEI; and (6) pure PEI. This interphase morphology is new in scientific literature because the material of the co-cured layer is already present in the thermoset resin system. Note that between (1) and (2) there can be a small region where the M18 resin is disturbed slightly by the co-cured layer, resulting in a morphology formed by NG and SD, assuming the original morphology is formed by SD only, or by NG and SD but with a different ratio of NG/SD. This would imply that the region where the M18 resin was disturbed by the co-cured PEI layer is slightly larger. However this is omitted since morphology formation is not the objective in this research.

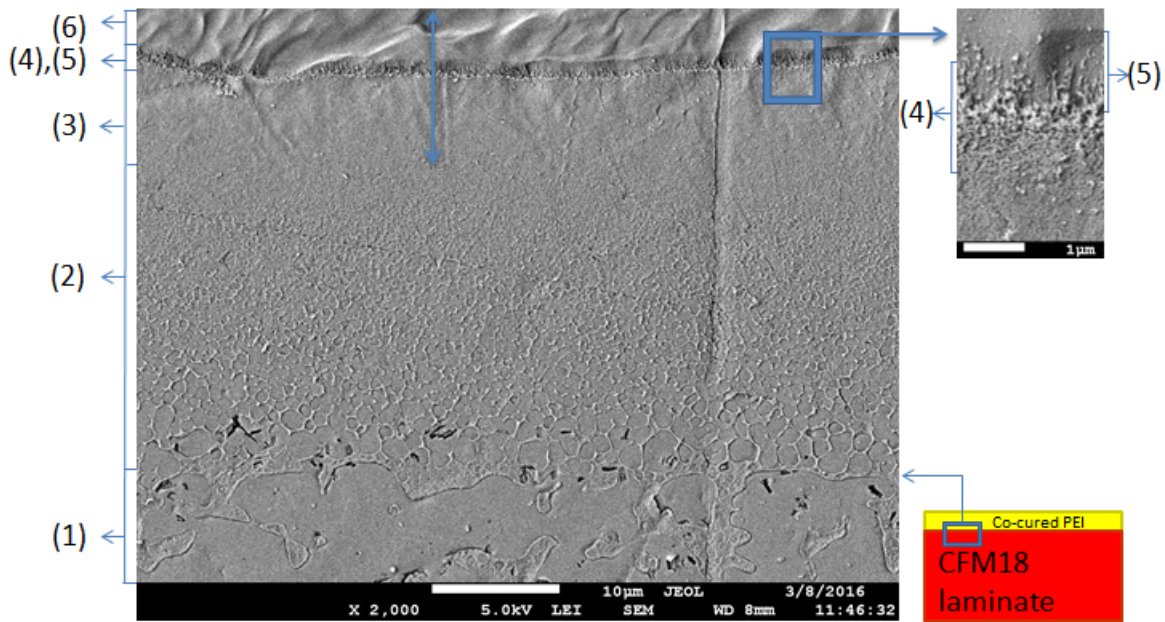


Figure 3.10: SEM image of the M18/PEI interphase, indicating the different zones: (1) pure M18, (2) M18 with increased PEI content, (3) PEI with increased epoxy content, (4) epoxy flow front, (5) dark band and (6) pure PEI. The double arrow indicates the approximate location of the original co-cured PEI layer.

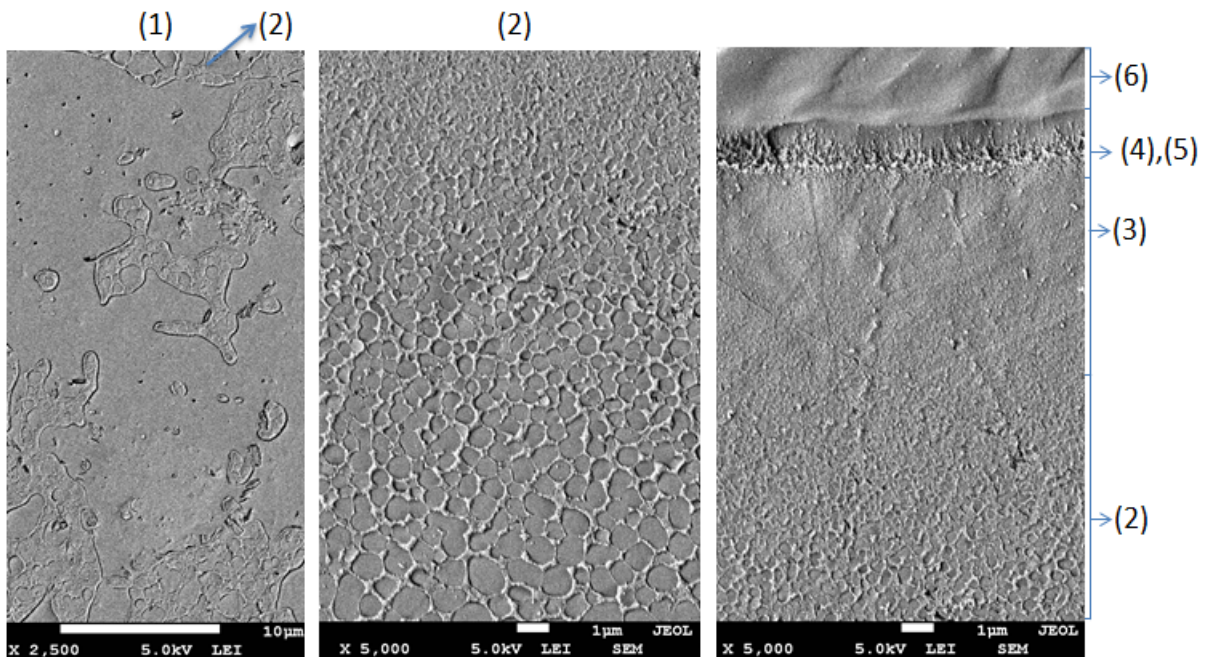


Figure 3.11: Detailed SEM images of the M18/PEI interphase. Left figure is detail from zone (1), also displaying the start of zone (2). Centre figure is detail from zone (2). Right figure are zones (3), zones (4) and (5) which are partly overlapping and zone (6).

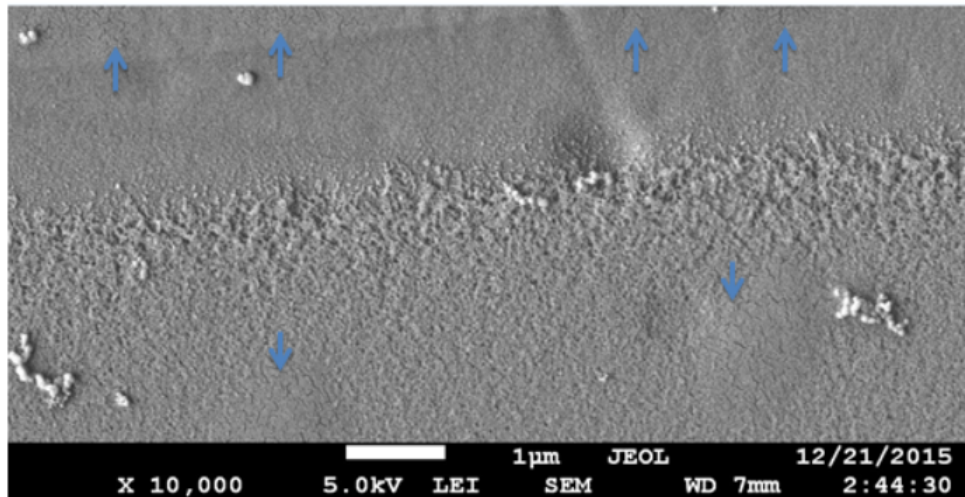


Figure 3.12: Microcracks, present in zone (6) pure PEI and (3) PEI with increased epoxy content, probably caused by the etching.

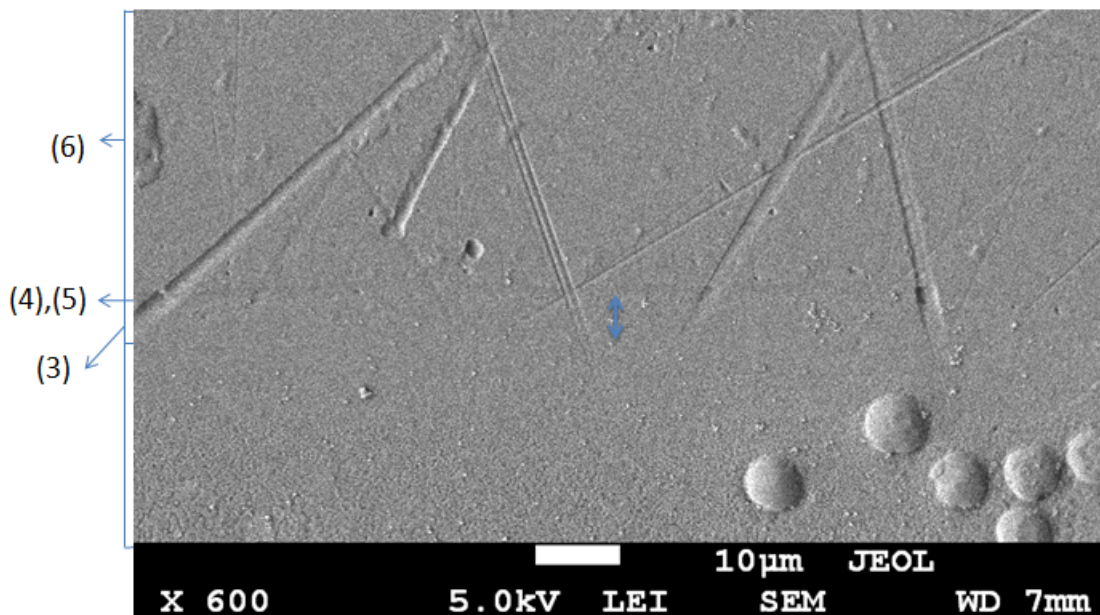


Figure 3.13: Scratches, present in zones (3) to (6), caused by polishing. The double arrow shows the region where the scratches extend into zone (3).

The size of the total interphase, zones (2) to (5) varies, this is visible in Figure 3.14, the border between black and grey have a non-linear shape. The smallest interphase measured with SEM was $30\mu\text{m}$. Large interphases are also present, dispersed epoxy spheres of zone (2) have been found between the first and second ply of the laminate, although this is an exception. Zone (3) is typically $7\text{--}10\mu\text{m}$. Zone (4) and (5) are nearly constant in size, respectively $2\mu\text{m}$ and $1.5\mu\text{m}$. Carbon fibre seems to be a physical barrier for diffusion since the sizes of zone (2) and (3) are typically smaller near carbon fibre. This is well visualised in Figure 3.15. The smallest interphase size is found near fibres that are close to the co-cured layer. Direct comparison of the interphase size with literature is challenging due to the different case discussed here. The conditions that influence the size of the interphase compared to other cases in literature are that the M18 resin is B-stage before cure, which reduces the diffusion speed of the epoxy [28], the thermoplastic in the M18 resin slows down cure kinetics [28], which increases time for diffusion, the different combination of chemical components and lastly the fact that the resin contains the same thermoplastic as the co-cured layer. But it is certain that the interphase is significantly smaller than the interphases discussed in literature. For example A-stage DGEBA-MCDEA

epoxy, cured with DDS, MCDEA and PEI yielded an interphase of $330\mu\text{m}$ [28]. A most fair comparison of size is comparing the diffusion distance of the epoxy into the thermoplastic. The example reports $21\mu\text{m}$ which is about double the size of zones (3) and (4) in our case.

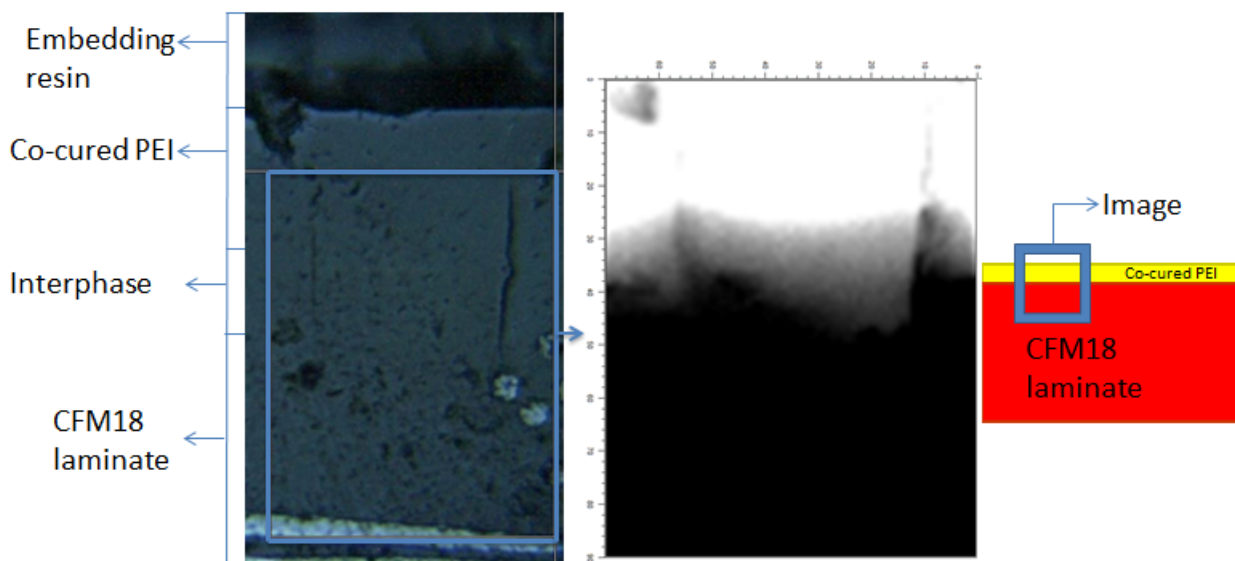


Figure 3.14: Left image: Raman spectroscopy false colour image, indicating two height measurements of the width of the interphase. The image displays a greyscale where the concentration from PEI varies approximately between pure PEI (displayed white) and 20% PEI (the PEI concentration blended in the M18). Right image: optical microscopy image of the scan performed with Raman spectroscopy. The border between black and grey is not a straight line, indicating varying interphase sizes.

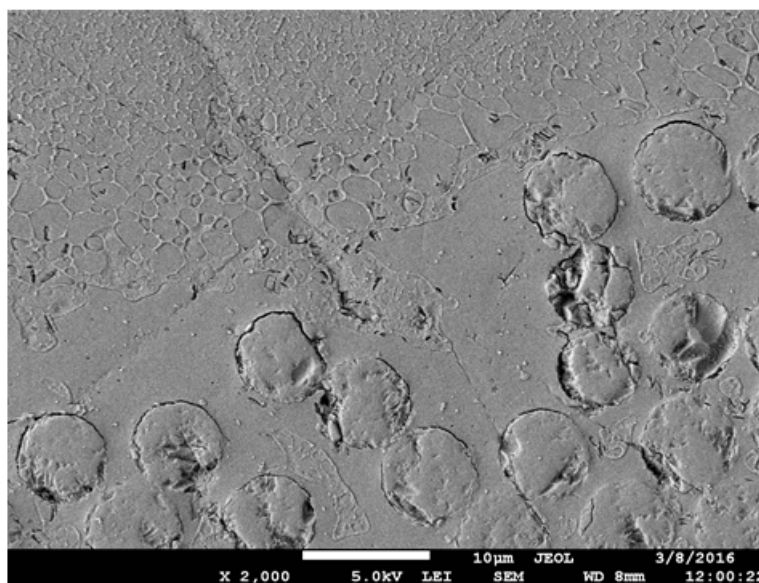


Figure 3.15: Fibres can form a physical barrier to the diffusion, zone (1) can be persistent in between the fibres.

3.2.4. Conclusion

M18 co-cured with PEEK does not form an interphase while M18 co-cured with PEI does form an interphase, as expected. The interphase morphology changes gradually according to the local PEI concentration.

3.3. Influence of welding on the thermoplastic-thermoset connection

The co-cured PEI or PEEK layer is used as a fusible layer for ultrasonic welding to a carbon reinforced PEEK adherend. The CFM18PEEK adhesive interface is maintained after welding, see Figure 3.16 which is not always the case as shown in the research of Nicolás Morillas [9] and discussed in subsection 1.1.2.

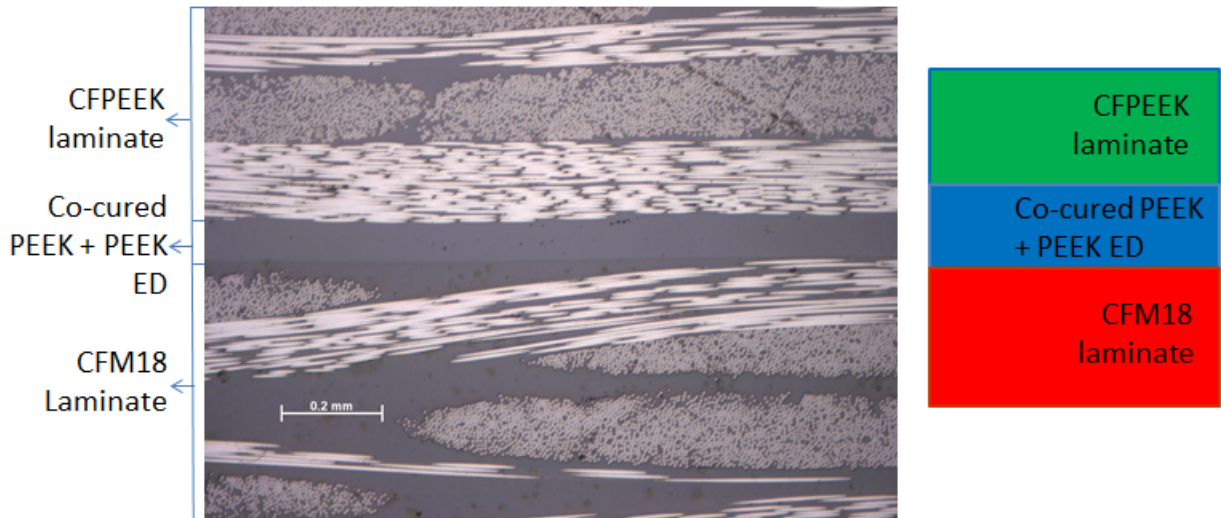


Figure 3.16: Optical microscopy image of the interphase region in CFM18PEEK/PEEK/CFPEEK joint.

SEM images of the post-weld interphase between CFM18 and PEI show that the interphase can be disrupted by the welding process. The interphase can be partially transported out of the weld zone with the flow of the energy director. This is evidenced by some of the zones which are absent and the sudden transition of the interphase type of morphology to pure PEI, zone (6), originating from the co-cured layer and energy director. Figure 3.17 shows that interphase zone (4) only remains partially present, the interphase was affected in the upper zone. In Figure 3.18 the interphase is terminated in the border region of zone (2) and zone (3), the deeper regions of the interphase. The interphase is not affected in every location, also undisturbed interphases are found. The high magnifications with SEM makes it challenging to have a clear overview over the whole overlap. Based on the observations an estimation is given on the length of the weld overlap that is affected. It is believed that the interphase is 45% undisturbed, 45% affected in the upper zones of the interphase as in Figure 3.18 and 10% affected as in the deeper zones as in Figure 3.18. Figure 3.18 is the deepest the interphase was affected. Since the PEI locally displaced part of the interphase it must have been above its T_g , temperatures above the T_g allow molecular intermingling (healing) to occur [4] when pure PEI is in close contact with the PEI domains in the interphase. Upon healing the materials become indistinguishable from the bulk [17], which is the case seen here between the PEI from the interphase and the PEI from the co-cured layer/ED, thus the fusion bond is re-obtained in the locations where the interphase is affected by the welding. Despite the temperature the epoxy domains do not display any change, seemingly not degraded in the short time at high temperature during welding. This is possible because very short times can potentially prevent the occurrence of degradation [16].

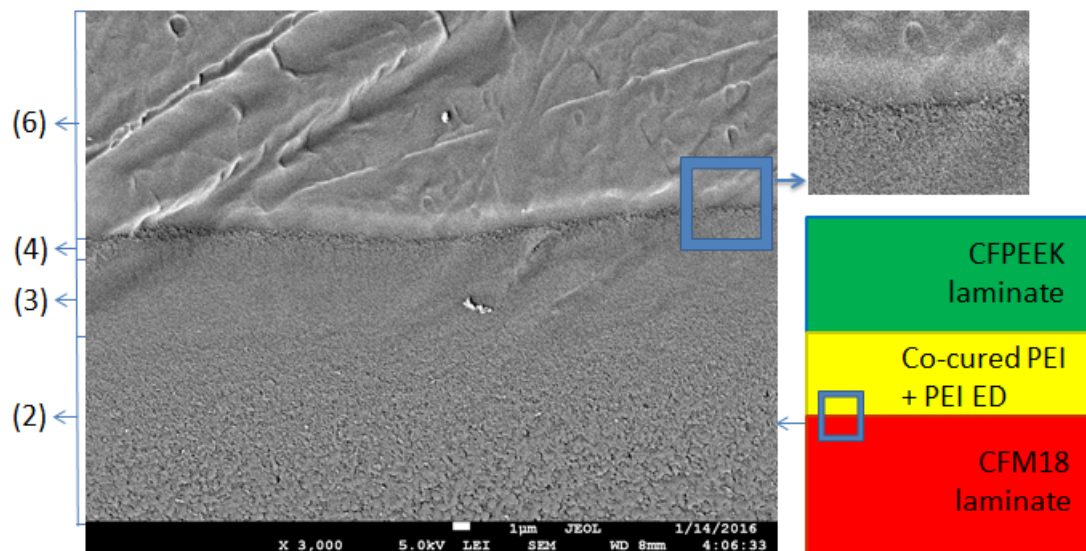


Figure 3.17: SEM image of the interphase region in CFM18PEI/PEI/CFPEEK joint. A detail of an image is presented in the top right corner, the interphase terminates in the epoxy diffusion front, zone (4).

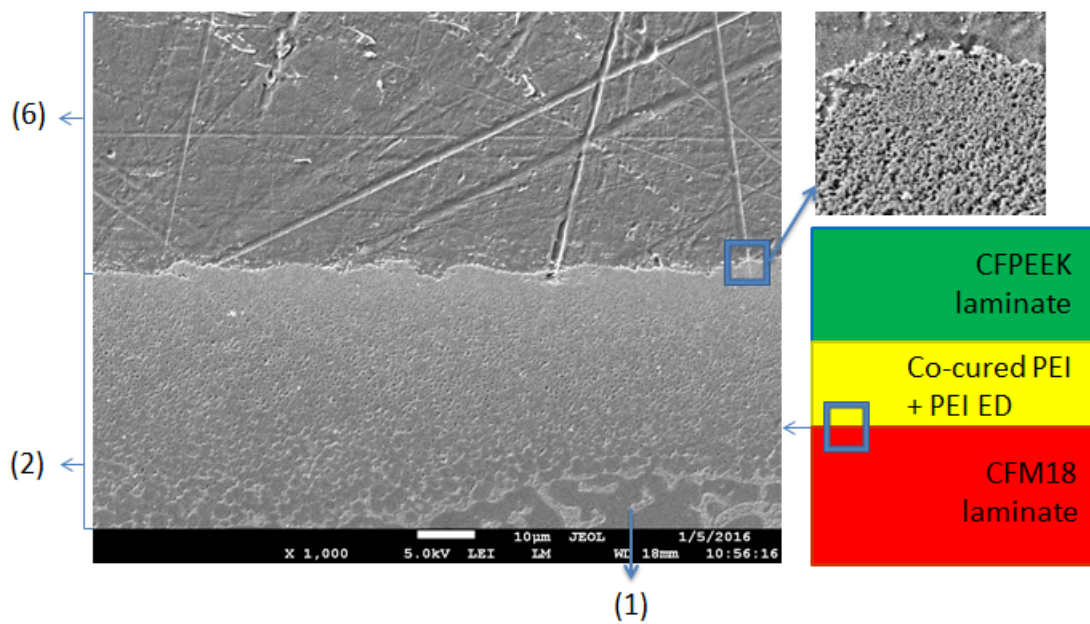


Figure 3.18: SEM image of the interphase region in CFM18PEI/PEI/CFPEEK joint. A detail of an image is presented in the top right corner, the interphase terminated the neighbourhood of the border between zone (2) M18 with increased PEI content and (3) the PEI region with increased epoxy content.

3.4. Co-curing of stiffeners

Instead of co-curing a neat resin layer as performed previously, structural elements like a carbon reinforced PEI stiffener can be directly co-cured. A demonstrator was created by co-curing a carbon fibre reinforced L stiffener to a CFM18 skin, see Figure 3.19. Optical microscopy, Figure 3.20 and SEM Figure 3.21 show the successful formation of the interphase between the two structural elements.

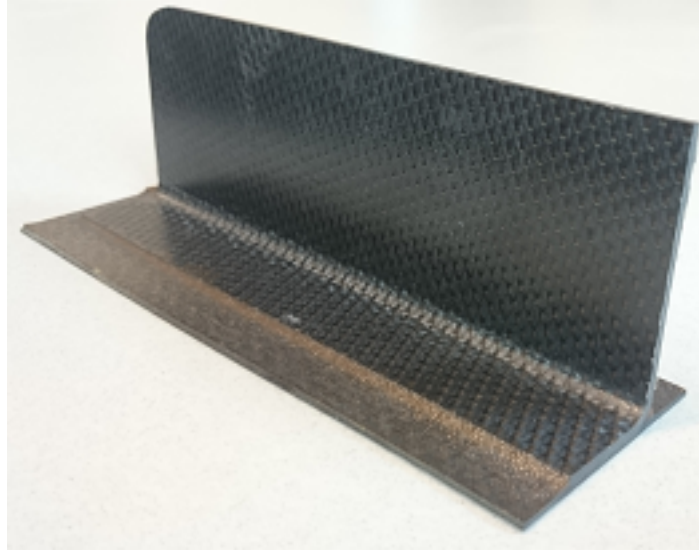


Figure 3.19: Demonstrator of a carbon reinforced PEI stiffener co-cured to a CFM18 skin.

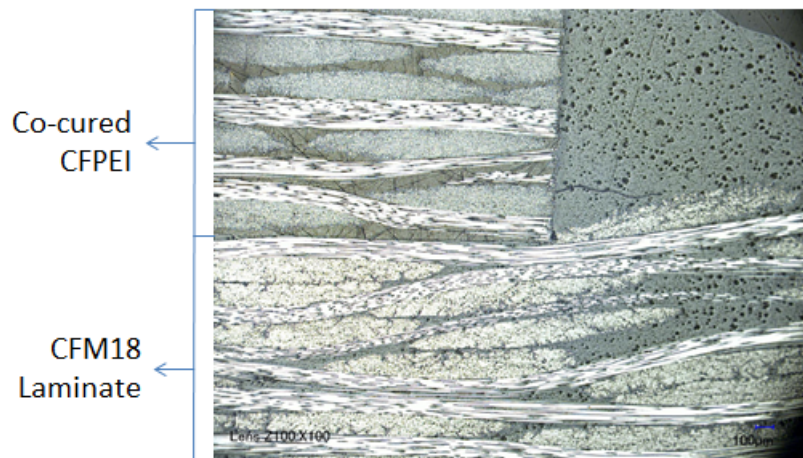


Figure 3.20: Optical microscopy image of the carbon reinforced PEI stiffener co-cured to a CFM18 skin. The upper laminate is the flange of the stiffener, which sank into the CFM18 skin below during cure.

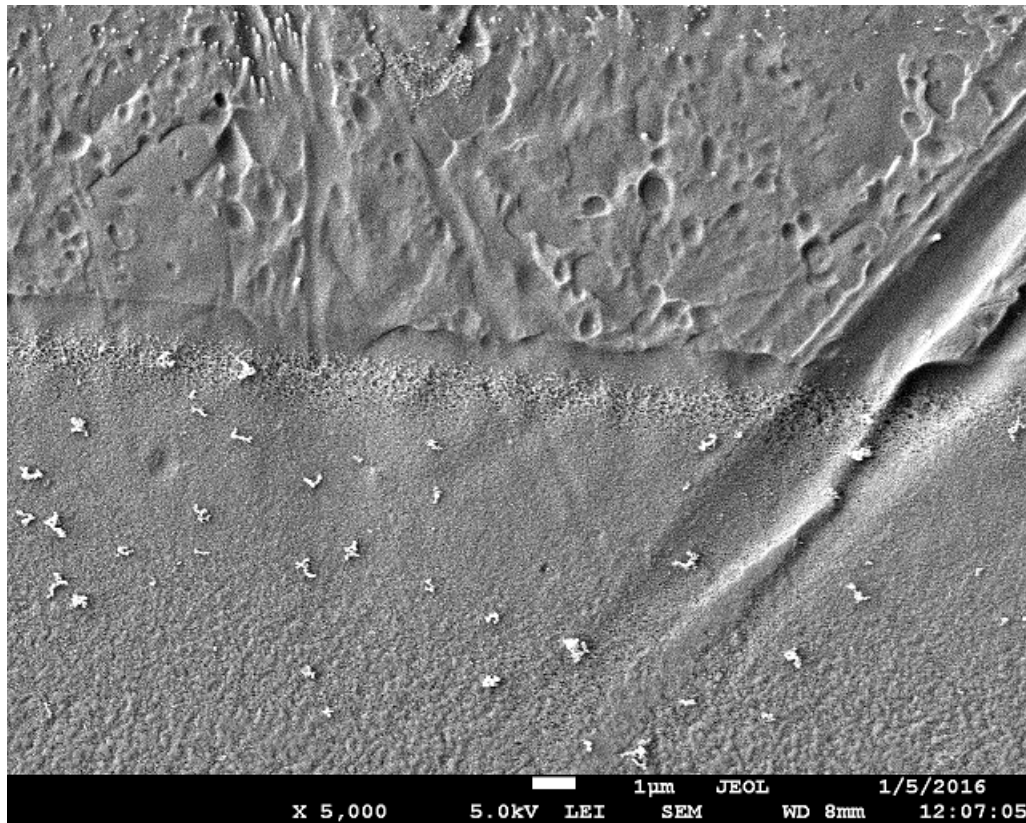


Figure 3.21: SEM image of the interphase between the carbon reinforced PEI stiffener co-cured to a CFM18 skin of Figure 3.19.

3.5. Conclusion

The objective of this thesis is to work towards welding PEEK attachments to a thermoset skin. This chapter investigated the thermoset-thermoplastic connection of a co-cured layer before and after ultrasonic welding. Both co-cured materials, PEEK and PEI show promising results. The adhesive interface between CFM18 and PEEK is maintained after welding, which is not always the case as shown in the research of Nicolás Morillas [9]. The certification issues encountered with adhesive joints remain in this type of joint. This is not the case for CFM18 with PEI, where an interphase was formed. The interphase is affected after welding at some locations but the fusion bond remains successful through the whole weld overlap. Future research should include other chemically compatible material combinations. Now that successful welding is established it is time to look at the performance of the joints.

4

Welded joints

4.1. Determination of optimum welding parameters

This section details the reasoning for choosing the welding parameters. The main goal is to avoid degradation of the thermoset material. Degradation is avoided by minimizing the welding time [5]. The largest force/highest amplitude combination available within the power limit of the welder is 2000N and 73.4 μ m peak-to-peak welding amplitude. The determination of the optimum sonotrode displacement uses the theory by Villegas [43], which states that the power curves generated by the welding system can be related to physical occurrences and strength development in the joint. The power curve can be divided into 5 stages, these stages are also related to a typical sonotrode displacement range. A sonotrode displacement that terminates the weld in stage 4 is chosen since this will yield the highest LSS [43]. Villegas et al. [5] stated that degradation results in dry fibres, due to sublimation of the resin during welding. SEM image shows that there is no degradation with these optimum parameters, evidenced by the fibres still coated in resin, Figure 4.1.

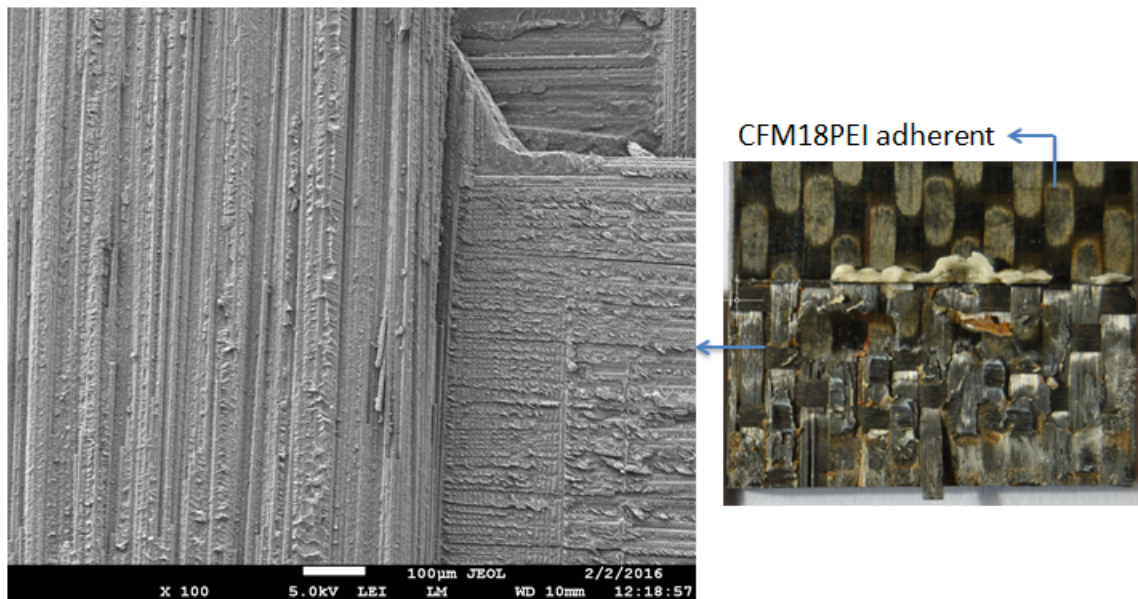


Figure 4.1: Fractured CFM18PEI/PEI/CFPEEK joint (An CFM18 adherend with a cocured PEI film, welded with a PEI energy director to a CFPEEK adherend). Joint was welded with 2000N and 73.4 μ m peak-to-peak welding amplitude and sonotrode displacement of 0.16mm. Fibres are still coated in resin, indicating no resin degradation.

4.2. Performance at dry/RT

Several different joint types were created with the available materials. The lap shear values are reported in Table 4.1 and Figure 4.3. Joint nomenclature: laminate X/ energy director Y/ laminate Z, as in Figure 1.9. For example the CFM18PEI/PEI/CFPEEK joint has a CFM18 laminate with a PEI co-cured layer, welded with a PEI energy director to a CFPEEK laminate. "Conventional" joints containing only carbon fibre reinforced thermoplastic laminates (TP/TP) are created as a general reference to put the performance of the remaining joints in perspective. The main focus is on the joints containing both a thermoplastic and a thermoset laminate (TP/TS). It will be demonstrated that the co-cured layer technique can also be used for joining laminates with only carbon fibre reinforced thermoset laminates in the joint (TS/TS). The last type of joint was cured instead of welded. This provides a reference on the performance of the joint without the influence of welding. The joint was created by placing a 50 μ m PEI layer between two CFM18 laminates which have the same lay-up as the welded samples, followed by curing the whole assembly, see Figure 4.2.

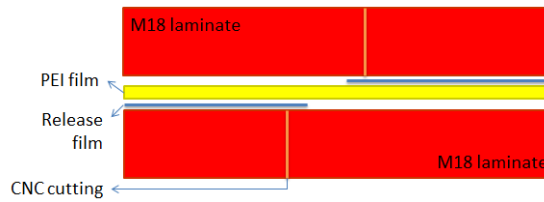


Figure 4.2: Lay-up of the cured lap shear joint.

Table 4.1: Summary of the apparent lap shear strength of all the joints with statistical significance. Weld parameters are welding force [N], peak-to-peak welding amplitude [μ m] and sonotrode displacement [mm]. Thickness of the used energy director is 0.25mm in all cases.

Joint type	Weld parameters		LSS \pm Stdev. [MPa]	Weld time \pm Stdev [ms]
	Force [N]; Amplitude [μ m]; Displacement [mm]			
CFPEEK/PEEK/CFPEEK	2000; 73.4; 0.15		43.00 \pm 3.41	629 \pm 44
CFPEEK/PEI/CFPEEK	2000; 73.4; 0.22		42.38 \pm 4.49	550 \pm 37
CFM18PEI/PEI/CFPEEK	2000; 73.4; 0.16		28.62 \pm 2.27	421 \pm 48
CFM18PEEK/PEEK/CFPEEK	2000; 73.4; 0.16		29.95 \pm 2.74	516 \pm 40
CFM18PEI/PEI/CFM18PEI	2000; 73.4; 0.16		24.85 \pm 1.59	479 \pm 57
CFM18PEEK/PEEK/CFM18PEEK	2000; 73.4; 0.16		23.61 \pm 0.87	450 \pm 43
CFM18/PEI/CFM18 cured joint	Cure cycle		26.53 \pm 0.72	NA

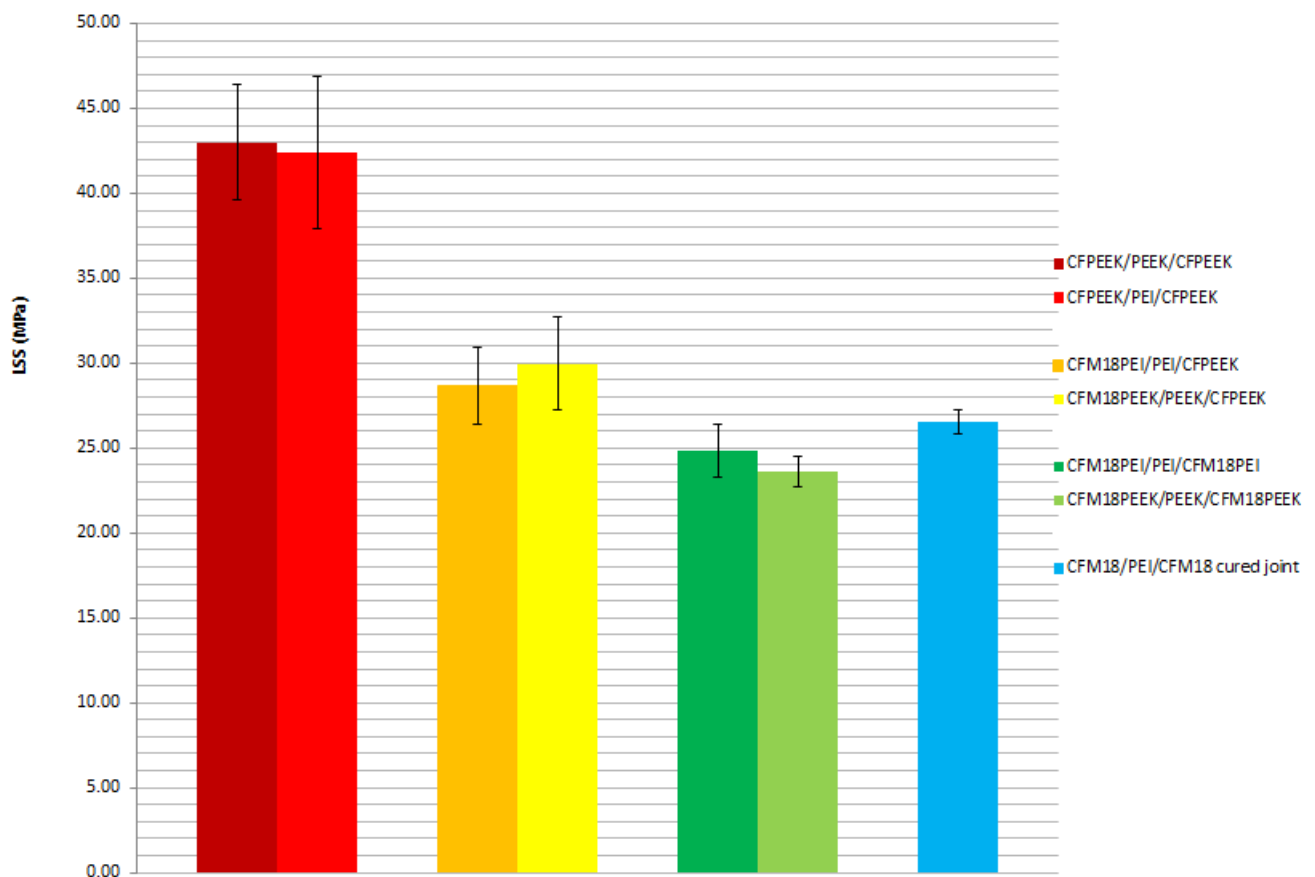


Figure 4.3: Summary of the apparent lap shear strength of all different types of joints with statistical significance.

The results in Figure 4.3 show that the thermoplastic only joints display the highest LSS. Compared to TP/TP joints the LSS of the TP/TS joint are significantly lower, attributed to the fact that the TP/TS joints mainly fail in the epoxy laminate, discussed later, while the TP/TP joints can only fail in the TP laminate. Within the TP/TS group the joints with a PEI co-cured layer, which formed an interphase between the thermoplastic interlayer and the thermoset material and the joint with the UV treated PEEK co-cured layer, forming an adhesive interface, are of comparable strength. The interphase formation could have weakened the M18 resin by changing the local concentration ratios of the M18 resin components, but this is not reflected in the LSS or the fracture surface, discussed in the next paragraph. The TS/TS joints have the lowest LSS. The TS/TS CFM18PEI/PEI/CFM18PEI joint is the most similar to the cured reference joint. The difference in LSS is only 1.68MPa. Which suggests that the welding does not induce any major damage or disadvantageous influence to the strength performance of the joint. Note that the cured joint has a overlap length of 13.18 mm, St. Dev. 0.21 mm, compared to the 12.7 mm of the welded overlap. The cured joint has a uniform 'bondline' thickness of 50 μ m (original thickness of PEI layer) while the 'bondline' thickness of the welded joint is non-uniform, no measurement for this joint is available. Maximum bondline thickness for CFPEEK/PEI/CFPEEK joint is 97 μ m, welded with the same amplitude and force but with a displacement of 0.15 instead of the 0.16mm for the TS/TS joint. No explanation is available for the reduction in strength when comparing TP/TS to TS/TS. SEM inspection of the fracture surface of the TS/TS and TP/TS joints did not indicate degradation. Cross-sectional microscopy or SEM of the TS/TS welding can maybe provide an additional clue but this type of joint is not the focus of this research. All the fracture surfaces display unwelded zones, visible in Figure 4.7. These unwelded areas are addressed in section 4.3.

The TP/TS joints fail mainly in the first ply of the epoxy laminate when an epoxy laminate is present, see Figure 4.4 and Figure 4.5. When the fracture path moves away from the first ply it can be located in all the materials present between the second ply of each laminate. The evaluation of the fracture path for the CFM18/PEI interphase requires a higher magnification, the interphase boundaries are not clearly visible in optical microscopy images and are therefore not sufficient to see if the path truly is outside the interphase. Figure 4.6 illustrates that the fracture path does not stay within the interphase. This indicates that the interphase formation and the welding did not produce a weak area in the joint.

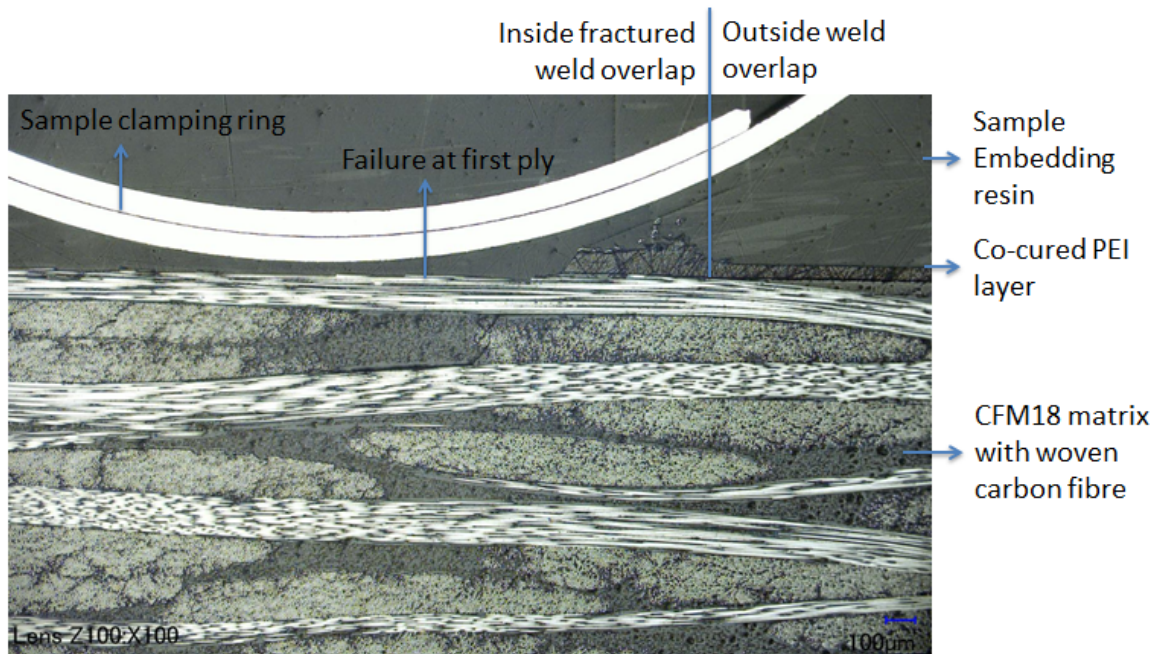


Figure 4.4: Illustrative image of fractured CFM18/PEI/PEI/CFPEEK joint. Only the CFM18 laminate is displayed. Fracture occurred mainly in the first ply of the CFM18 laminate.

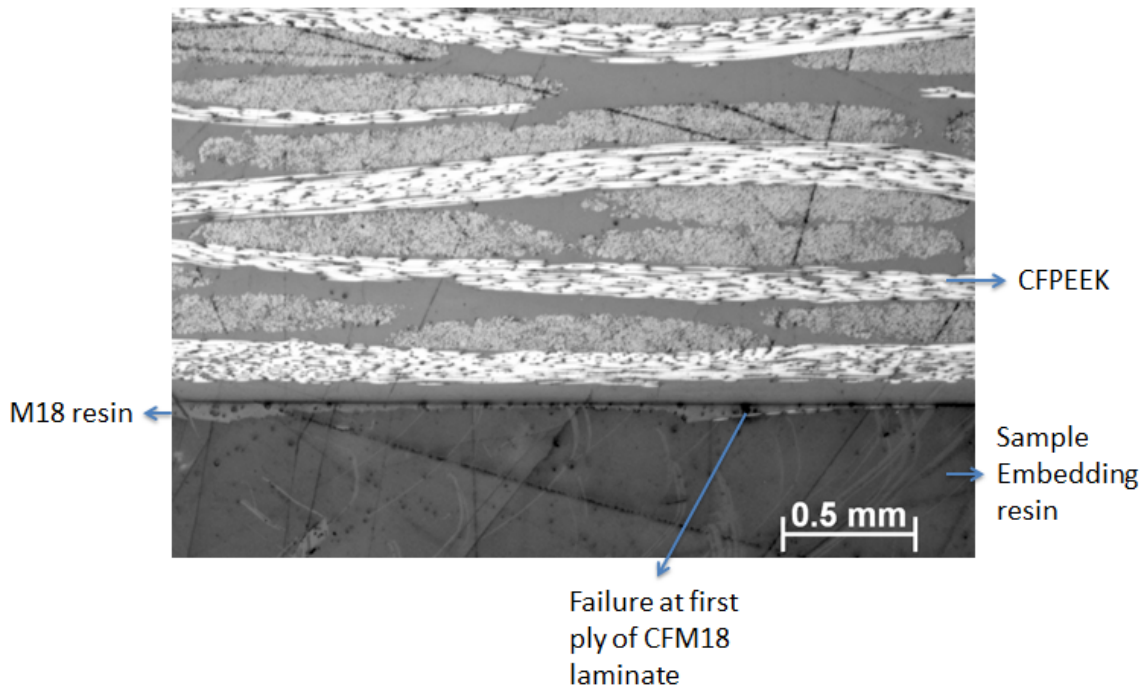


Figure 4.5: Illustrative image of fractured CFM18PEEK/PEI/CFPEEK joint. Only the PEEK laminate is displayed. Fracture occurred mainly in the first ply of the CFM18 laminate. No voids are present due to welding as discussed in section 3.3.

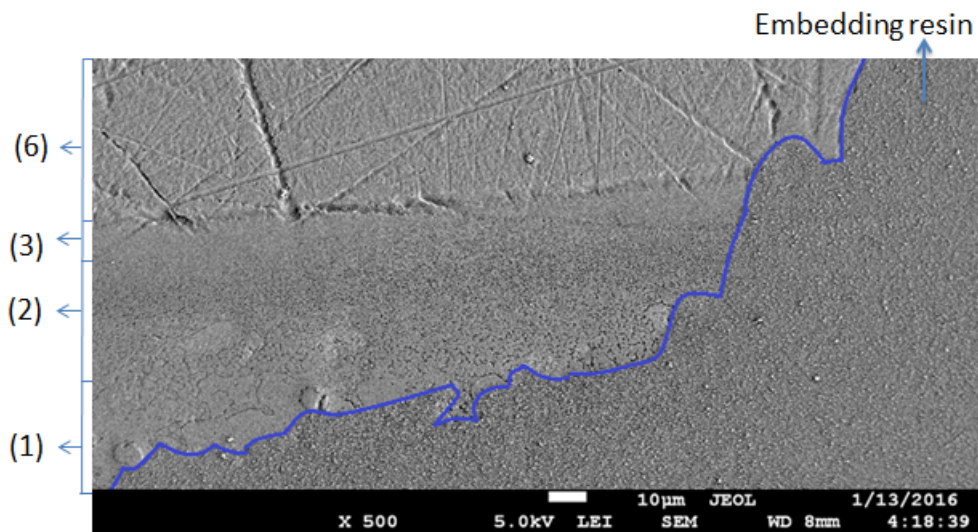


Figure 4.6: Illustrative image of a fractured CFM18PEI/PEI/CFPEEK joint. This image illustrates that the fracture is not preferentially in the co-cured layer. The fracture path, highlighted by the blue line, does not linger in the interphase zones. Visible zones are (1) pure M18, (2) M18 with increased PEI content, (3) PEI with increased epoxy content and (6) pure PEI.

4.3. Reducing the unwelded zones

The joints welded with the optimum processing parameters discussed in section 4.1 display unwelded areas in the weld overlap, see Figure 4.7. The cause is related to the optimum welding parameters. High force/amplitude welding parameters result in shorter heating times [5] (which we desired to minimize degradation) and less energy input. It also increases the flow of heated energy director material out of the weld overlap. Therefore the high force/amplitude settings reduce the available heat for fusion bonding the materials.

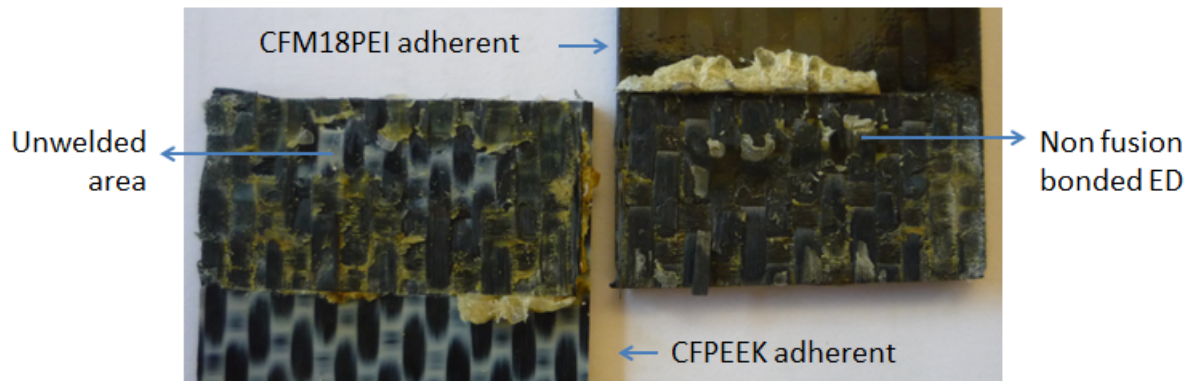


Figure 4.7: Fractured CFM18PEI/PEI/CFPEEK reference joint (An CFM18 adherent with a cocured PEI film, welded with a PEI energy director to a CFPEEK adherent). Joint was welded with 2000N and 73.4 μ m peak-to-peak welding amplitude and sonotrode displacement of 0.16mm. The joint displays an unwelded area in the centre of the weld overlap.

Two strategies to reduce the unwelded area are explored: reducing the welding parameters and adapting the energy director. First solution is to reduce the welding force to decrease flow and thus retain heat. The reference joints, CFM18PEI/PEI/CFPEEK yielded 28.62MPa, see Table 4.1. If the welding force for the same joint type is reduced from 2000N to 1000N (other weld parameters used are 73.4 μ m welding amplitude and sonotrode displacement 0.16mm) the LSS value is maintained at 28.45MPa, St.Dev 2.23MPa. The change in unwelded area of the untreated (reference) joints reported here was limited. This weld setting was also used for another test where samples are immersed in MEK, the fracture surfaces of these samples shown in Figure 4.8 shows that unwelded area can be reduced with this strategy. Note that Figure 4.8 is a joint that was tested in MEK immersion, discussed later in subsection 4.4.2. The method is successful for small overlaps but probably not sufficiently effective for reducing larger unwelded zones in larger overlaps.

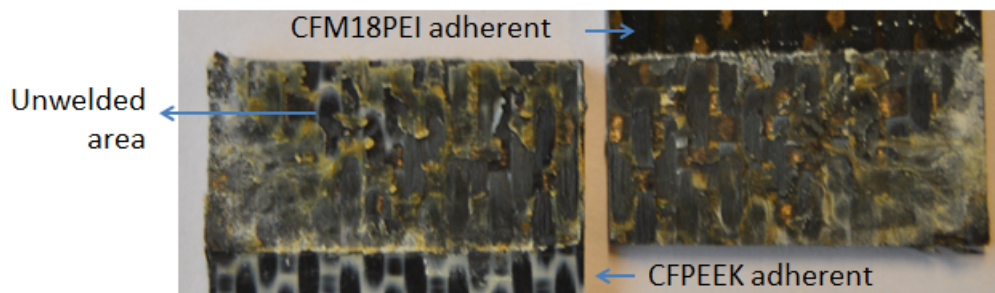


Figure 4.8: Fractured CFM18PEI/PEI/CFPEEK joint (An CFM18 adherent with a cocured PEI film, welded with a PEI energy director to a CFPEEK adherent). Joint was welded with 1000N and 73.4 μ m peak-to-peak welding amplitude and sonotrode displacement of 0.16mm. The joint displays a smaller unwelded area in the centre of the weld overlap compared to Figure 4.7. The joint was immersed for 12 days in MEK, which changes the type of fracture, discussed in subsection 4.4.2.

A solution thought to be more appropriate for larger overlaps that resemble real applications is adapting the energy director to create more free edges. The free edge should trigger additional surface friction in the centre of the overlap, thereby reducing the unwelded area. For the joint in this research an additional free edge is created by changing the regular flat energy director to a flat energy director with a slit, Figure 4.9. This creates a free edge in the centre of overlap where the unwelded areas are typically located. The weld is successfully fusion bonded at the edge but right next to the edge the unwelded areas remain. The joints are welded with 2000N welding force, 73.4 μ m welding amplitude and 0.16mm sonotrode displacement, the slit is approximately 1mm wide. The joints yielded an LSS of 28.88MPa with St.Dev. 0.87MPa, which is comparable to the aforementioned 28.62MPa reference. It is recommended to create more free edges for large overlaps.

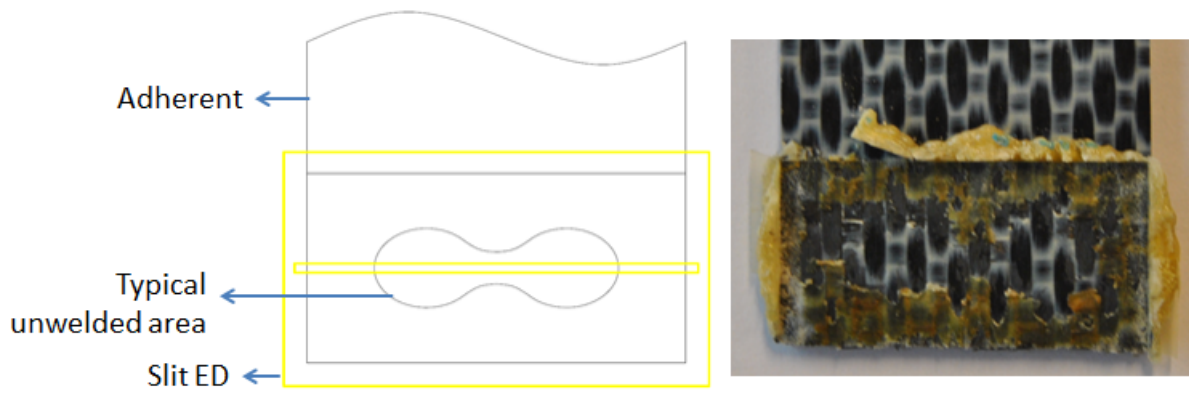


Figure 4.9: On the left a schematic of the use of a slit energy director (ED), as positioned in relation to a typical unwelded zone. On the right an example of an unwelded zone.

4.4. Performance in a manufacturing environment

4.4.1. Exposure to water

Joints are immersed in 70°C water for one week. This represents a worst case scenario for immersed C-scan inspection during production. Selection of time and temperature is on the basis of practicality given equipment and time available within the constraint of a worst case scenario. Previous experience with co-cured PEEK layers in the welding research group at the faculty of Aerospace engineering at the TU Delft indicated that it is possible to experience a change in the fracture surface after exposure to moisture, where the co-cured PEEK layer releases from the epoxy laminate instead of failure within the epoxy laminate. Release of the surface treated PEEK layer did not occur in this research within the time and temperature window of this test. The PEI containing joints can absorb significant moisture because of their amorphous nature. This could influence the strength and location of failure. But also no strength drop or change of failure type was observed. All the tested joints retained their LSS value and type of fracture, Figure 4.10. A limited amount of samples were also exposed for the prolonged time of one month, but no drop in strength or change in fracture surface was observed.

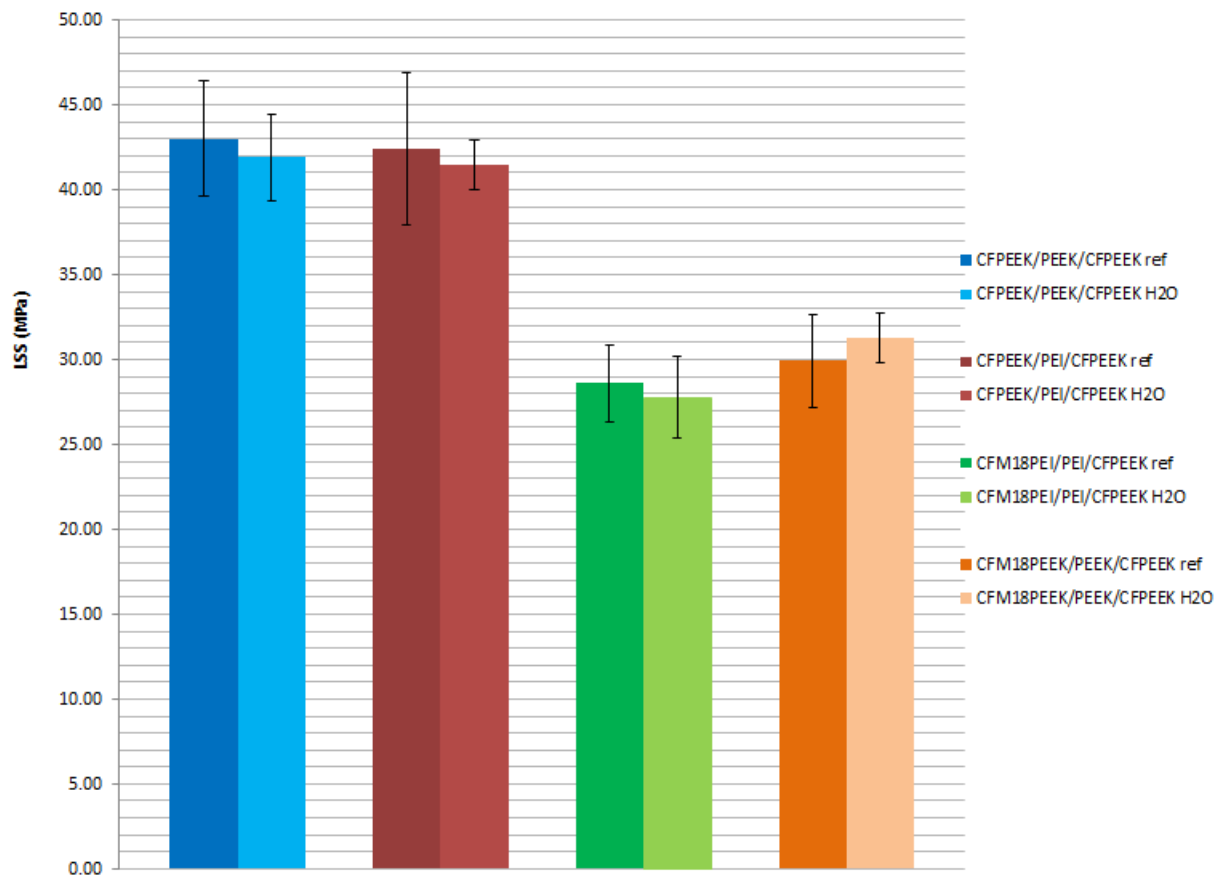


Figure 4.10: Summary of the apparent lap shear strength of the joints immersed in 70°C water for 1 week, displayed together with the respective reference case without treatment. Samples were kept immersed until testing.

4.4.2. Exposure to MEK

MEK is used as a cleaning solvent on cured composite parts. Conversations with Fokker showed that a one hour immersion of material in MEK is a standard test to indicate sensitivity of amorphous thermoplastic materials to MEK exposure. A PEI resin film was submerged in MEK for 48 hours, the PEI swelled, becoming soft and pliable. This material is thus of interest to test MEK exposure. The joints are modestly affected after one hour of exposure to MEK. After 12 hours the strength drop is significant, it drops from 28.45MPa to 20.75 MPa, see Figure 4.11, Table 4.2. Some of the failure within the epoxy ply of the reference joint is changed to cohesive failure within the PEI. This is best visible when comparing Figure 4.13 with Figure 4.12. Figure 4.12 is a joint immersed for 12 days in MEK, the joint displays more cohesive failure then the reference joints such as Figure 4.13, where the failure occurs in the laminate itself, evidenced in the figure by the fibre sticking out of the laminate. The CFM18PEEK/PEEK/CFPEEK joint was not affected after an hour of MEK immersion, as expected. No 12 day immersion was performed due to lack of samples.

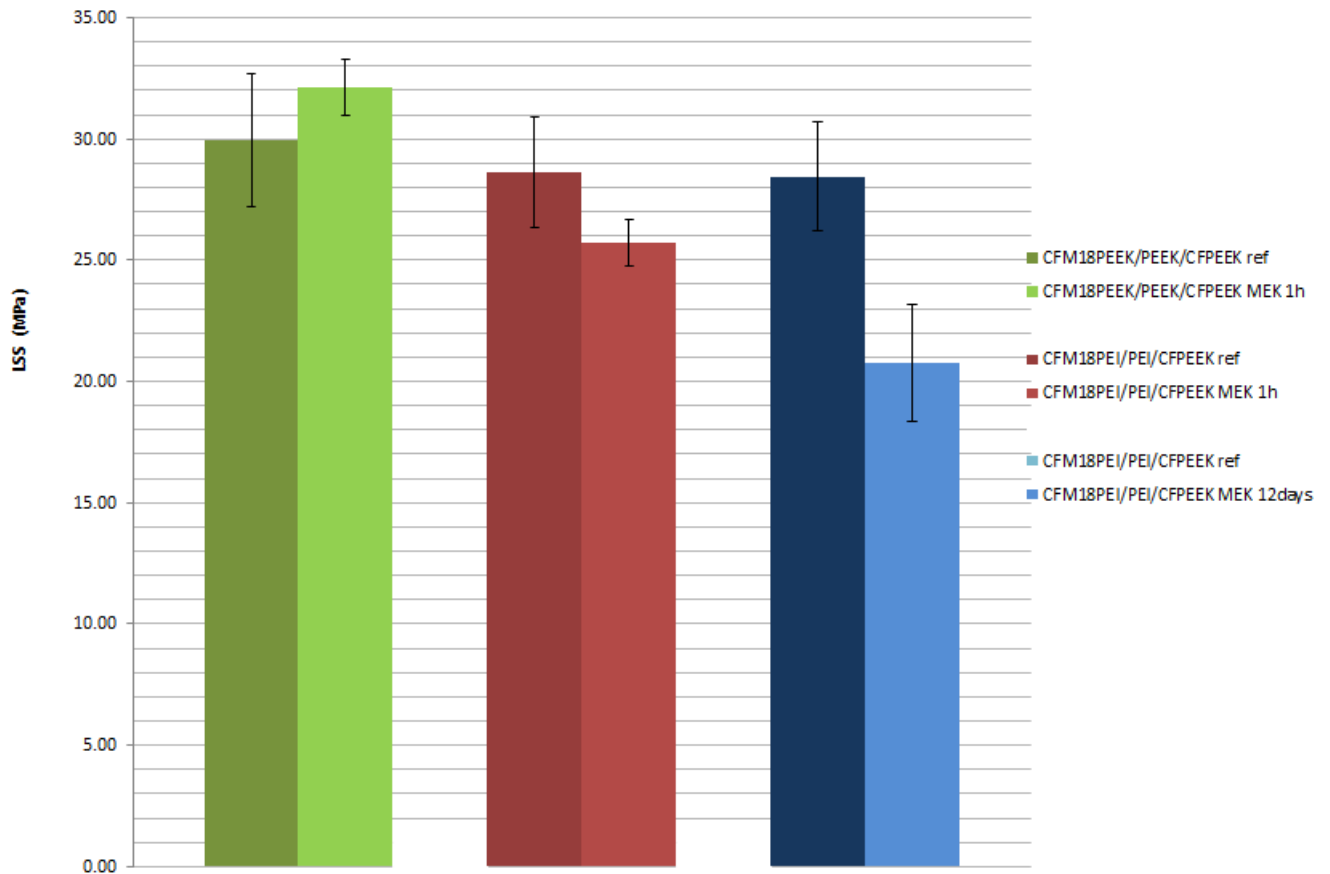


Figure 4.11: Summary of the apparent lap shear strength of the joints immersed in MEK, displayed together with the reference case without treatment. Samples were kept immersed until testing.

Table 4.2: Summary of the apparent lap shear strength of all the joints with statistical significance. Weld parameters are welding force [N], peak-to-peak welding amplitude [μm] and sonotrode displacement [mm]. Thickness of the used energy director is 0.25mm in all cases.

Joint type	Weld parameters Force [N]; Amplitude [μm]; Displacement [mm]	LSS \pm Stdev. [MPa]	Weld time \pm Stdev [ms]
CFM18PEI/PEI/CFPEEK ref	2000; 73.4; 0.16	29.95 \pm 2.74	516 \pm 40
CFM18PEEK/PEEK/CFPEEK 1h MEK	2000; 73.4; 0.16	32.15 \pm 1.16	456 \pm 47
CFM18PEI/PEI/CFPEEK ref	2000; 73.4; 0.16	28.62 \pm 2.27	421 \pm 48
CFM18PEI/PEI/CFPEEK 1h MEK	2000; 73.4; 0.16	25.71 \pm 0.96	552 \pm 46
CFM18PEI/PEI/CFPEEK ref	1000; 73.4; 0.16	28.45 \pm 2.23	612 \pm 141
CFM18PEI/PEI/CFPEEK 12d MEK	1000; 73.4; 0.16	20.75 \pm 2.42	638 \pm 101

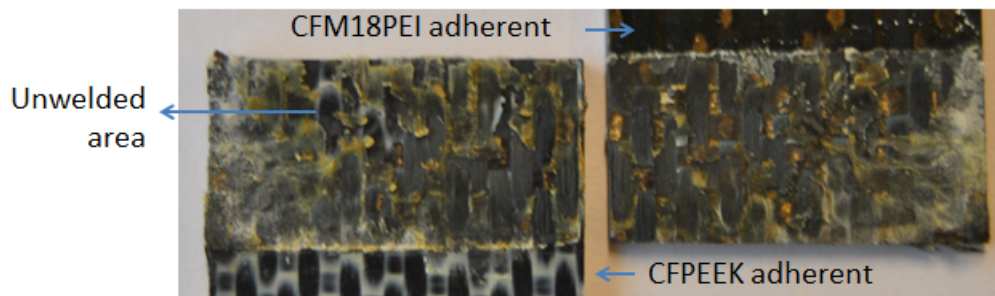


Figure 4.12: Fractured CFM18PEI/PEI/CFPEEK joint (A CFM18 adherend with a cocured PEI film, welded with a PEI energy director to a CFPEEK adherend). Joint was welded with 1000N and 73.4 μm peak-to-peak welding amplitude and sonotrode displacement of 0.16mm. The joint was immersed for 12 days in MEK, which changes the type of fracture.

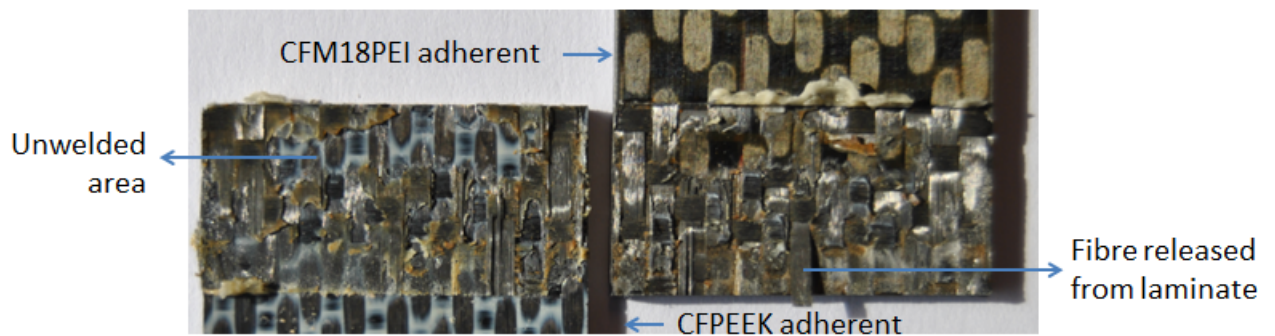


Figure 4.13: Fractured CFM18PEI/PEI/CFPEEK joint (A CFM18 adherend with a cocured PEI film, welded with a PEI energy director to a CFPEEK adherend). Joint was welded with 2000N and 73.4 μm peak-to-peak welding amplitude and sonotrode displacement of 0.16mm. This image clearly shows that there is fracture within the adherend, evidenced by the carbon fiber pointing outward.

4.4.3. Exposure to contaminants

Fusion bonded joints are supposed to require less surface preparation before processing than adhesively bonded joints [2]. However no data in literature to confirm this is available. A small trial experiment is performed with one contaminant, PF-SR Sealant Remover & Surface Cleaner, used in the welding lab at the Aerospace faculty in the TU Delft to clean the sonotrode. CFM18 laminates are wiped with a cloth soaked in PF-SR right before welding. The time between welding and surface treatment is less than one minute, surface looked optically wet before welding. Results are in Figure 4.11. Only two joints per joint type were tested. Considering this is a gross contamination of the surface the drop in strength is limited but significant. These are promising results and should be explored further in future research.

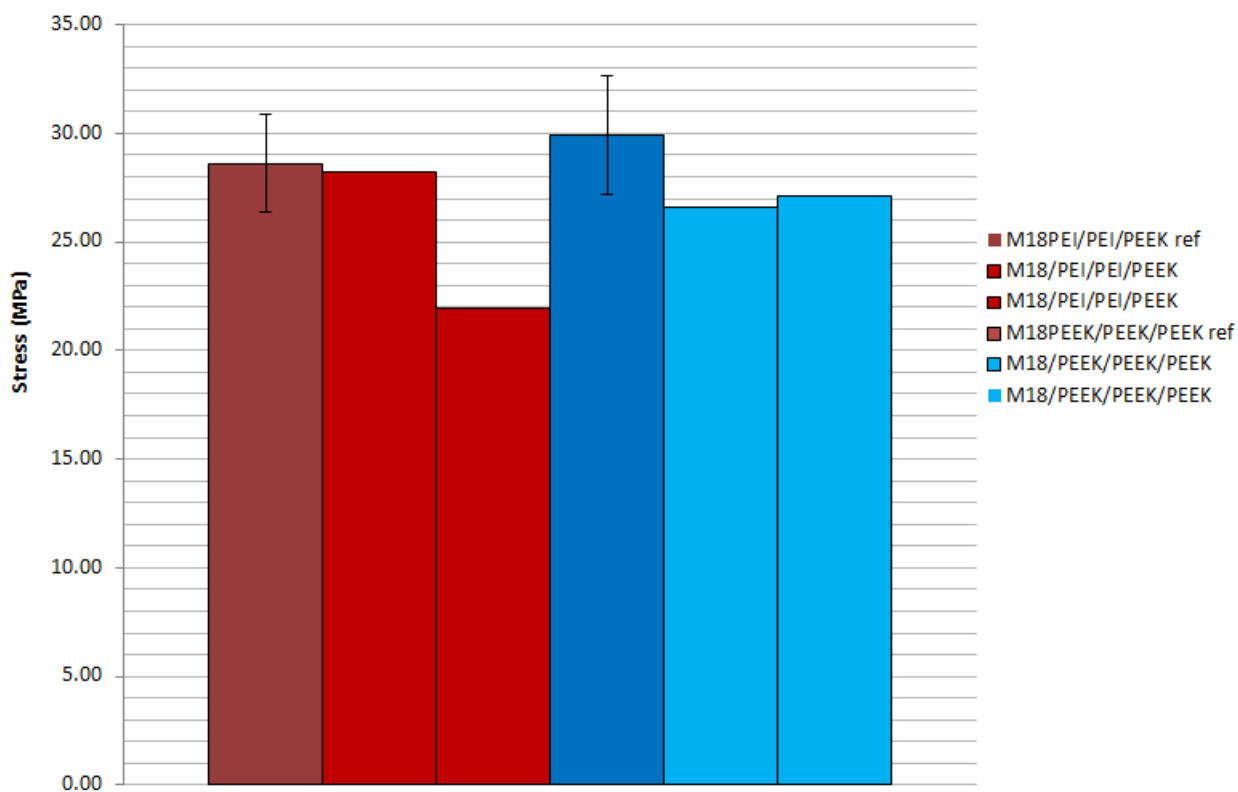


Figure 4.14: Summary of the apparent lap shear strength of the joints immersed in MEK, displayed together with the reference case without treatment. Samples were kept immersed until testing.

4.5. Conclusion

This chapter investigated the performance of ultrasonically welded joints that contain both thermoplastic and thermoset materials. RT/D TP/TS reference joints yielded 28.62MPa for the CFM18PEI/PEI/CFPEEK joint and 29.95MPa for the CFM18PEEK/PEEK/CFPEEK joint. Unwelded zones were obtained with the optimum processing parameters, these can be addressed by reducing the welding settings or changing the energy director. The last approach is recommended for larger overlaps in future work. The strength of the joints is retained after prolonged exposure to moisture. No loss of adhesion between the thermoplastic PEEK co-cured layer and the CFM18 thermoset laminate was observed. Exposure in MEK influenced the joint performance of the TP/TS joint containing PEI. Here a lower LSS was obtained and the amount of failure within the epoxy laminate was decreased, changing it to a cohesive failure in the PEI. Finally a preliminary test addressing the claim that fusion bonded joints require less surface preparation than adhesive joints was tested, yielding promising results that confirm the claim. It must be stressed that all the tests only aimed to simulate worst cases in a manufacturing environment and not a service environment. Aging tests and LSS tests at temperatures other than room temperature or at different moisture levels should be performed on these joints.

III

Conclusions and recommendations

5

Conclusion

The long-term goal in the research area where to this thesis contributes is to fusion bond a carbon fibre reinforced PEEK bracket to a carbon fibre reinforced thermoset skin for aerospace applications. This thesis worked towards this goal by investigating the possibility to use an initially miscible, co-cured interlayer as fusible surface for the fusion bonded joint. An initially miscible co-cured layer has the potential of forming a gradient interphase, where the concentration of the materials gradually changes from the thermoset resin to the thermoplastic resin. One alternative is the use of a non-miscible, surface treated co-cured layer, where the layer remains attached to the thermoset through an adhesive interface. The use of a miscible co-cured layer can potentially avoid the certification challenges of adhesive joints while providing an alternative to mechanical fastening of cured thermoset aerospace structures.

After literature review the aerospace grade M18 thermoset resin, reinforced with carbon fibre in combination with a thin co-cured interlayer of PEI Ultem 1000 from SABIC was selected as an initially miscible system. As a non-miscible system the CFM18 material is co-cured with a PEEK interlayer from Vitrex, which is surface treated to generate an adhesive interface between the two materials. This research investigated methods to identify and inspect the interlayer and the connection between the interlayer and the thermoset resin. Three complementary techniques were selected, optical microscopy, Raman spectroscopy and scanning electron microscopy (SEM). Optical microscopy could provide a general overview of the interlayer, useful for inspecting welded joints. Raman spectroscopy provides a general overview of the interphase formed in the initially miscible system, or the absence of an interphase in the non-miscible system. Finally SEM revealed the morphology of the M18 resin and the interphase, which enables the researcher to identify the presence or absence of an interphase and to inspect the interphase in detail. PEI does not have any optical contrast with the M18 resin, therefore the co-cured PEI layer and the PEI used as toughening within the M18 resin had the same appearance as the cured epoxy when untreated. Solvent etching of the PEI containing samples created contrast and topographical differences with the epoxy by partially dissolving a superficial layer of PEI.

Thermal degradation of the thermoset resin is a challenge for fusion bonding since the temperatures required for fusion bonding exceed the maximum temperature of the thermoset resin. A fast heating method was selected, namely ultrasonic welding. This provided sufficiently short heating times so that the maximum temperature and time at elevated temperatures remained limited, thereby preventing degradation. The requirement of short heating times resulted in aggressive welding conditions, which could potentially damage the connection between the interlayer and the thermoset resin. The non-miscible system used in this research was not affected due to the welding. The miscible system was partially affected, detailed inspection of the interphase with SEM showed that in some areas within the weld overlap the interphase can be transported out of the weld zone with the flow of the energy director. In the affected locations the PEI from the energy director re-obtained a fusion bond with the PEI domains in the interphase. Despite the effect of welding the interphase did not become a weak area, as evidenced by the fracture path.

The joints with the interphase between PEI and CFM18 have similar dry/RT performance as the joints with the adhesive interface between UV-treated PEEK and CFM18. Both joint types fail mainly within the thermoset laminate. The amorphous nature of the PEI raises questions on the capability to withstand the effects

of moisture and solvents. These conditions are seen during commercial manufacturing since structures are often C-scanned, using water, and cleaned with cleaning solvents such as MEK. Therefore the joints were exposed to moisture for a week at elevated temperature, which did not affect the joint performance. MEK had a slight effect on the joints containing the amorphous PEI. Extended exposure made the effect more significant. This should be taken into account when creating cleaning procedures in a commercial manufacturing setting for these type of joints.

This research shows that fusion bonding can be used for thermoset laminates using interphase forming interlayers. The welding process affects the interphase locally but the fusion bond is maintained in the whole weld overlap. The certification difficulties encountered in adhesive bonding can therefore potentially be avoided if an interphase forming material combination is chosen for the interlayer and the thermoset resin. Surface treated interlayers can also be used, but certification of these joints for use in aerospace remains a challenge.

6

Recommendations

The following topics for future research are suggested:

- upscaling of the welding process so that real structures can be welded in the future;
- hot/wet aging of the joints to test their performance during service;
- test other interphase forming material combinations, since this interphase is only established for one material combination;
- a thorough evaluation of the sensitivity of welded joints to contaminations on the welding surface, this can prove that the welding process is more tolerant to contaminants than adhesive bonding.

Bibliography

- [1] S. Deng, L. Djukicb, R. Paton, and L. Yea, *Thermoplastic epoxy interactions and their potential applications in joining composite structures a review*, Composites Part A: Applied Science and Manufacturing Volume 68, Pages 121-132 (2015).
- [2] C. Ageorges, L. Ye, and M. Hou, *Advances in fusion bonding techniques for joining thermoplastic matrix composites: a review*, Composites: part A, Vol 32, No. 6, pp. 839-857 (2001).
- [3] T. Kruse, *Bonding of cfrp primary aerospace structures: overview on the technology status in the context of the certification boundary conditions addressing needs for the development*, in *The 19th International Conference on Composite Materials* (2013).
- [4] A. Christine, R. McCullough, and R. Pitchumani, *An analysis of mechanisms governing fusion bonding of thermoplastic composites*, Journal of thermoplastic composite materials Vol. 11 (1998).
- [5] I. Fernandez Villegas and P. Vizcaino Rubio, *On avoiding thermal degradation during welding of high-performance thermoplastic composites to thermoset composites*, (2015).
- [6] A. Firas, M. Gilbert, K. Georgina, F. Bronwyn, Paul, and J. Pigram, *Adhesion of polymers*, Progress in Polymer Science 34 (2009).
- [7] G. Jacaruso, G. Davis, and A. McIntire, *Method of making thermoplastic adhesive strip for bonding thermoset composite structures*, United States Patent No. 5264059 (1993).
- [8] P. Vizcaino Rubio, *Hybrid Welding of Thermoset and Thermoplastic Composites*, Master's thesis, TU Delft (2014).
- [9] M. Nicolas Morillas, *Hybrid welding of thermoset and thermoplastic composites adhesion improvement*, Master's thesis, Delft University of Technology (2015).
- [10] R. Don, S. McKnight, E. Wetzel, and J. Gillespie, *Application of thermoplastic resistance welding techniques to thermoset composites*, Society of Plastic Engineers (1994).
- [11] M. H. C.R. Beyler, *Thermal decomposition of polymers*, SFPE Handbook of Fire Protection Engineering (1995).
- [12] R. Dan, V. Cristian-Dragos, R. Liliana, and M. Oana Maria, *Thermal Degradation of Polymer Blends, Composites and Nanocomposites* (Springer, 2015).
- [13] Hexcel, *Hexply m18 product datasheet*, .
- [14] M. Hou, A. Beehag, and Q. Yuan, *Welding techniques for polymer or polymer composite components*, US Patent 8 790 486 (2012).
- [15] M. Van Toren, *Method for bonding a thermoplastic polymer to a thermosetting polymer component*. International Patent Application No. WO2012 161569A1 (2012).
- [16] E. Wetzel, R. Ron, and J. Gillespie, *Modelling thermal degradation during thermoplastic fusion bonding of thermoset composites*. Proceedings of the 52nd annual technical conference ANTEC (1994).
- [17] D. Grewell and A. Benatar, *Welding of plastics: fundamentals and new developments*, International Polymer Processing (2007).
- [18] A. Pereira da Costa, E. Cocchieri Botelho, M. Leali Costa, N. Eiji Narita, and J. Ricardo Tarpani, *A review of welding technologies for thermoplastic composites in aerospace applications*, Journal of Aerospace Technology and Management (2012).

- [19] C. Ageorges and L. Ye, *Resistance welding of thermosetting composite/thermoplastic composite joints*, Composites Part A: Applied Science and Manufacturing (2001).
- [20] M. Hou, *Fusion bonding of carbon fiber reinforced epoxy laminates*, Advanced Materials Research Vol. 626, pp. 250-254 (2012).
- [21] S. McKnight, B. Fink, V. Monnar, P. Bourban, J. Manson, D. Eckel, and J. Gillespie, *Processing and characterization of welded bonds between thermoset and thermoplastic composites*, Army Research Laboratory Aberdeen Proving Ground MD 21005-5096 (2001).
- [22] M. Hou, *Thermoplastic adhesive for thermosetting composites*, Materials Science Forum, Vols 706-709, Pages 2968-2973 (2012).
- [23] D. Grewell, A. Benatar, and J. Park, *Plastics and Composites Welding Handbook* (Hanser Publishers, 2003).
- [24] M. Tolunay, P. R. Dawson, and K. Wang, *Heating and bonding mechanisms in ultrasonic welding of thermoplastics*, Polymer Engineering & Science (1983).
- [25] I. Fernandez Villegas, *In situ monitoring of ultrasonic welding of thermoplastic composites through power and displacement data*, Journal of Thermoplastic Composite Materials (2013).
- [26] A. Levy, S. Le Corre, and I. Fernandez Villegas, *Modeling of the heating phenomena in ultrasonic welding of thermoplastic composites with flat energy directors*, Journal of Materials Processing Technology Volume 214, Issue 7 (2014).
- [27] D. A. McCarville and H. A. Schaefer, *Processing and joining of thermoplastic composites*, ASM Handbook, Volume 21: Composites (2001).
- [28] B. Lestriez, J. Chapel, and J. Gerard, *Gradient interphase between reactive epoxy and glassy thermoplastic from dissolution process, reaction kinetics, and phase separation thermodynamics*, Macromolecules, 34 (5), pp 1204-1213 (2001).
- [29] L. Vandt, M. Hou, M. Veidt, R. Truss, M. Heitzmann, and R. Paton, *Interface diffusion and morphology of aerospace grade epoxy co-cured with thermoplastic polymers*, in *28th Congress of the International Council of the Aeronautical Sciences* (2012).
- [30] L. H. Sperling, *Interpenetrating polymer networks*, Advances in chemistry (1994).
- [31] M. T. Heitzmann, M. Hou, M. Veidt, L. J. Vandt, and R. Paton, *Morphology of an interface between polyetherimide and epoxy prepreg*, Advanced Materials Research, Vols 393-395, pp. 184-188 (2011).
- [32] G. Rajagopalan, K. Immordino, G. Jr., J.W., and S. McKnight, *Diffusion and reaction of epoxy and amine in polysulfone studied using fourier transform infrared spectroscopy: experimental results*, Polymer Volume 41, Issue 7, pp. 2591-2602 (2000).
- [33] L. Utracki and C. Wilkie, *Polymer Blends Handbook* (Springer, 2014).
- [34] B. A. Miller-Chou and J. Koenig, *A review of polymer dissolution*, Progress in Polymer Science Volume 28, Issue 8, Pages 1223-1270 (2003).
- [35] Olympus, *Contrast in optical microscopy*, <http://www.olympusmicro.com/primer/techniques/contrast.html>.
- [36] P. Gilmore, R. Falabella, and R. Laurence, *Polymer polymer diffusion effect of temperature and molecular weight on macromolecular diffusion in blends of poly(vinyl chloride) and poly(ε-caprolactone)*, Macromolecules.13(4) 880-883 (1980).
- [37] G. Crevecoeur and G. Groeninckx, *Binary blends of poly(ether ether ketone) and poly(ether imide), miscibility, crystallization behavior, and semicrystalline morphology*, Macromolecules Vol.24, 1190-1195 (1991).
- [38] www.matweb.com, *Unreinforced peek datasheet*, .

-
- [39] L. McKague, *Thermoplastic resins*, ASM Handbook, Volume 21: Composites (2001).
- [40] J. Vig, *Uv/ozone cleaning of surfaces*, Journal of Vacuum Science & Technology A (1984).
- [41] I. Mathieson and R. Bradley, *Improved adhesion to polymers by uv/ozone surface oxidation*, Int. J. Adhesion and Adhesives Vol. 16 29-31 (1996).
- [42] D. V. Sridhara Rao, K. Muraleedharan, and C. J. Humphreys, *Tem specimen preparation techniques*, Microscopy: Science, Technology, Applications and Education (2006).
- [43] F. V. I., *Strength development versus process data in ultrasonic welding of thermoplastic composites with flat energy directors and its application to the definition of optimum processing parameters*, Composites Part A: Applied Science and Manufacturing (2014).